Development of Improved dc Network Model for Contingency Analysis

by

Puneet Sood

A Thesis Presented in Partial Fulfillment
of the Requirements for the Degree
Master of Science

Approved November 2014 by the
Graduate Supervisory Committee:

Daniel Tylavsky, Chair
Vijay Vittal
Raja Ayyanar

ARIZONA STATE UNIVERSITY

December 2014

ABSTRACT

The development of new policies favoring integration of renewable energy into the grid has created a need to relook at our existing infrastructure resources and at the way the power system is currently operated. Also, the needs of electric energy markets and transmission/generation expansion planning has created a niche for development of new computationally efficient and yet reliable, simple and robust power flow tools for such studies. The so called dc power flow algorithm is an important power flow tool currently in use. However, the accuracy and performance of dc power flow results is highly variable due to the various formulations which are in use. This has thus intensified the interest of researchers in coming up with better equivalent dc models that can closely match the performance of ac power flow solution.

This thesis involves the development of novel hot start dc model using a power transfer distribution factors (PTDFs) approach. This document also discusses the problems of ill-conditioning / rank deficiency encountered while deriving this model. This model is then compared to several dc power flow models using the IEEE 118-bus system and ERCOT interconnection both as the base case ac solution and during single-line outage contingency analysis. The proposed model matches the base case ac solution better than contemporary dc power flow models used in the industry.

ACKNOWLEDGEMENTS

TABLE OF CONTENTS

LIST OF FIGURES

LIST OF TABLES

NOMENCLATURE

ac	Alternating current
B_{branch}	Branch susceptance matrix
B_{bus}	Bus susceptance matrix
b_{ij}	Susceptance of transmission line *ij*
C	Bus-Branch incidence matrix
CRR	Congestion Revenue Rights
C_S	Bus-branch incidence matrix for sub-network
dc	Direct current
ε	Tolerance value
EI	Eastern Interconnection
ERCOT	Electric Reliability Council of Texas
FACTS	Flexible *ac* transmission system
FTR	Financial Transmission Rights
g_{ij}	Conductance of transmission line *ij*
H	Susceptance of transmission line
HVDC	High voltage *dc*
ISF	Injection shift factor
J	Jacobian matrix
LODF	Line Outage Distribution Factor

NERC	North American Electric Reliability Corporation
NR	Newton Raphson
OPF	Optimal Power Flow
OTDF	Outage Transfer Distribution Factor
P_{flow}	Network branch power flow vector
P_{ij}	Power flow from bus i to bus j
P_{inj}	Bus injection vector
P_{ji}	Power flow from bus j to bus i
PQ bus	Non-generator bus or bus at VAR limit
PTDF	Power Transfer Distribution Factor
PV bus	Generator bus
P_G^i	Power generated at bus i
P_L^i	Load at bus i
P_{bus}^{shift}	Compensating bus power injection vector for phase shifter
P_{branch}^{shift}	Compensating branch power injection vector for phase shifter
P_k	Power flow over branch k
r_{ij}	Resistance of transmission line ij
RPS	Renewable Portfolio Standard
SCED	Security Constrained Economic Dispatch
SCUC	Security Constrained Unit Commitment

t_i	Transformer tap ratio
TLR	Transmission Loading Relief
TPL	Transmission Planning
Λ	Lambda matrix for main network
Λ'	Augmented lambda matrix
V_i	Voltage magnitude at bus i
V_j	Voltage magnitude at bus j
Λ_S	Lambda matrix for sub-network
WECC	Western Electricity Coordinating Council
x_{ij}	Reactance of transmission line ij
x_s	Reactance vector for sub-network
Y_{bus}	Admittance matrix
y_{ij}	Admittance of transmission line ij
z_{ij}	Impedance of transmission line ij
α_{k1}	Sending end loss compensation for branch k
α_{k2}	Receiving end loss compensation for branch k
γ	Single Multiplier for loss compensation
δ_i	Transformer phase shift angle
θ_i	Angle at bus i
θ_j	Angle at bus j

ϕ Power transfer distribution factor matrix

ϕ^{ac} *ac* power transfer distribution factor matrix

Φ^{dc} *dc* power transfer distribution factor matrix

Ψ Loss injection matrix

Δt Transacted power between two buses

1 INTRODUCTION

1.1 BACKGROUND

In 2012 the electricity sector was the largest source of greenhouse gas emissions in US, contributing 32% of the total greenhouse gas emissions, which is significantly better than the 40% share of electricity sector in 2009 for greenhouse gas emissions. Albeit the contribution of electricity sector towards greenhouse emissions has declined significantly but a lot needs to be done to further improve on clean energy [1]-[2]. The decline is the result of development of new environmental policies and federal tax incentives favoring integration of renewable resources into grid. Now more than 35 states have renewable energy targets in place [3]-[4]. In California, for example, as of April 2011, the renewable portfolio standards (RPS) requires California's electric utilities to derive 33% of their retail sales from eligible renewable energy resources by 2020 [5]. Because of governmental energy policies and incentives, the power industry is rapidly changing gears to accommodate renewable resources such as photovoltaics, wind in their energy portfolios and thus changing the traditional perspective of operation and design of power systems. Besides the changes in the generation in pattern, the 10-year planning summary prepared by Western Electricity Coordinating Council (WECC) indicated that there is a 14% expected rise in loads from 2009 to 2020, which is 1.2% compound annual growth rate [23]. However, to keep pace with the current trends in power systems, there is an urgent requirement to develop new tools to study the rapidly evolving power system.

It is a well-known that an ac power flow solution is more accurate than the corresponding dc solution for studies like power flow, contingency analysis. But the traditional Newton-Raphson (NR) algorithm used for the ac solution requires an iterative procedure which is quite time intensive and less appropriate for carrying out such studies where qualitative solution at an initial planning phase is of prime concern. Also, the interest in development of efficient dc power flow models has further intensified due to market applications (such as security–constrained economic dispatch (SCED), security-constrained unit commitment (SCUC)) where prices are a function of network congestions [6]. Conventionally, these approximate dc power flow models were used extensively to tackle convergence issues common to the full ac OPF, contingency screening, transmission loading relief and medium-to-long term transmission planning [6].

The objective of the work reported on here is to determine a dc model which takes into account branch resistance in the flow equations and which produces a better estimate of power flows during transmission line outages.

1.2 LITERATURE REVIEW

Network equivalencing, as the name suggests, is a procedure which reduces the complexity of the original model to create a simplified model either through reduction in system size or ease in computational requirements. Often these network equivalents are the results of dc approximations of ac network with an emphasis on preserving the original network properties as much as possible. Rich literature developed over the

2

years is descriptive of the myriad "dc power flow models" used for specific purposes like contingency analysis, market analysis. With the recent upsurge in the electric energy market applications stated earlier, interest has been renewed in the development of improved dc power flow models that better replicate the ac network model performance. The stimuli for such research is the desire for robustness, simplicity and speed of these models when used in the applications of interest.

The word "dc" in dc power flow comes from the use of old dc network analyzers, used to represent the series reactance as proportional series resistance and the current to represent the corresponding MW flow on the network [6]. The simplest version of dc power flow without any loss compensation, is a further simplification of fast decoupled power flow by completely neglecting Q-V equation and assuming constant 1 p.u. voltage magnitude. With these simplifications the dc power flow problem is reduced to solving a linear system of equations [7] and [21]. This "classical dc" series-reactance model is widely known as the original dc power flow method.

Variants of dc models are legion and their performance is affected by the loss compensation techniques invoked and branch susceptances selected. Furthermore, these dc models are inherently approximate and their accuracy is very system and case dependent yet they provide significant insight into system behavior under different operating scenarios [22]. This research work is focused on the development of dc network models from ac network models, therefore it is vital to study the impacts of assumptions (i.e. voltage magnitude 1 p.u., resistances neglected.) on the dc model's

accuracy. The theoretical implications of the assumptions made to derive a dc network model is well described in [8] while [9] – [11] and [22] discuss the effect of these assumptions on practical and realistic bulk energy systems. Reference [24] discusses the impact of flow controlling devices on dc power flow. Reference [26] presents the modification in the standard assumptions by introducing interval-valued dc power flow equations to overcome voltage and parametric uncertainties.

So-called dc power flow models have been segregated into different categories in literature. However, the more popular classification of these models include: incremental and non-incremental models. The non-incremental models are further categorized into hot start or state-dependent and cold start or state-independent dc models. The hot start dc models are based on the solved ac solution. In these type of models the series elements represent the power flow over the network and shunt elements model the loss injections. Therefore, these models match the ac solution losses at the base case. These types of models are used in real time SCED using a state estimator solution [12] and short / medium term planning studies. The other variant i.e. cold start dc models lacks a solved ac solution; thus the loss estimates are either neglected or an estimate is used that represent the losses as a percent of the net load. These type of models find utilization in the market based applications like financial transmission rights (FTR) / congestion revenue rights (CRR) [13] and long term planning studies.

Another category of models are known as the incremental models, which compute the incremental changes from a known ac or dc state [6]. These incremental models are sub-divided into sparse matrix models and sensitivity factor models. Sparse matrix models are based on the available base case ac/dc solution. The deviations from the base case (i.e. topological change – branch outage) are modeled as incremental changes in the problem formulation; this is performed by factor-updating in original formulation [6]. While in the sensitivity factor model, the sensitivity factors are a function of sparse dc network matrix and/or network solution. Computation of these sensitivity factors, like power transfer distribution factors (PTDFs), line outage distribution factor (LODF), outage transfer distribution factor (OTDF) is described in [14]. These sensitivity factors are widely used by system operators in the congestion modeling in market applications e.g., transmission loading relief (TLR) procedure, by providing fast approximations of the active power flow changes due to various system operations [20]. References [15] – [17] discuss the formation of network equivalents using the sensitivity factors and extending it further to obtain the reduced network models which tend to preserve network properties. References [18] – [19] provide an insight into the variation of sensitivity factors i.e., PTDFs with multiple loading scenarios across different systems.

References [16], [17] and [37] present network aggregation techniques applied to the classical dc formulations, but, for a complex network they suffer from the rank deficiency/numerical ill-conditioning problems. Also, when this technique is applied to a set of inconsistent PTDFs instead of consistent classical dc PTDFs the solution

becomes constraint dependent and yields different results for different constraints applied.

Often in deregulated electricity markets, the market participants, in the open access environment, want to maximize their profit, so they compete to obtain electrical energy from a cheap source, which may lead to congestion in the transmission network and affect system security and reliability [25]. This has increased the need to conduct dynamic security and reliability assessment on a real time basis. Therefore, contingency analysis plays an integral part of such a study.

Transmission planning (TPL) standards define reliable system performance following a loss of a single bulk electric element, two or more bulk electric elements, or following extreme events [27]. NERC [28] – [30], requires analysis of the following contingencies [27]:

- Resulting in a loss of a single element (Category B)
- Resulting in a loss of two or more elements (Category C)
- Extreme events forcing two or more elements removed or cascading out of service (Category D)

dc power flow models are frequently used to provide a insight when such an enormous number of cases must be taken under consideration.

1.3   RESEARCH OBJECTIVE

This research focuses on the development of an improved dc model which produces a better estimate of power flows during transmission line outages or contingencies. This report covers following areas:

1. Basic dc power flow formulation

2. Modeling of loss compensation in dc models

3. Introduction to PTDFs (both ac and dc)

4. Detailed development of a series element in the proposed dc model

5. Numerical issues in the development of this model

6. Comparison of the results of this model with other widely accepted dc models

1.4   THESIS OUTLINE

This thesis is divided into four additional chapters:

Chapter 2 introduces reader to general dc power flow model formulation and the underlying assumptions for development of such models.

Chapter 3 presents the new optimization based approach for the development of a series element of the proposed model.

Chapter 4 discusses the rank deficiency or ill-conditioned matrix issues encountered in the development of the proposed model.

Chapter 5 conducts the numerical illustration on 7-bus, IEEE-118 bus system and ERCOT interconnection to demonstrate the accuracy of this model compared to other more prevalent dc models.

Chapter 6 provides the summary of this research and future scope of work.

2 DC POWER FLOW MODEL FORMULATION

The power flow problem involves the solution of a non-linear system of equations using the traditional implicit methods like Newton-Raphson and Gauss-Seidel. In contrast, a dc power flow algorithm explicitly solves a linear system of equations, an equation set that is far more computationally efficient, i.e., non-iterative and low storage requirements. The advantages of speed and robustness offered by such models, makes the dc power flow an attractive option to pursue for several of the applications stated earlier.

In this chapter, the ac model for the power flow over a transmission line is first introduced and then the dc model assumptions are overlaid to derive the classical dc model formulation. A more generalized dc power flow model is then presented to the reader. Furthermore, cold-start and hot-start dc models with and without loss compensation respectively, are described in detail.

2.1   AC POWER FLOW MODEL FOR A TRANSMISSION LINE

A simplified ac network model for a transmission line connecting bus i and bus j is shown in Figure 2.1. The power flows on the branch at the sending end bus i and receiving end bus j are given by P_{ij} and P_{ji} respectively.

The active power flow from bus i to bus j under steady state conditions is described by the following power-flow equation:

$$P_{ij} = \text{Re}\left\{V_i \angle \theta_i \cdot \left[\left(V_i \angle \theta_i - V_j \angle \theta_j\right) \cdot (g_{ij} + j \cdot b_{ij})\right]^*\right\} \tag{2.1}$$
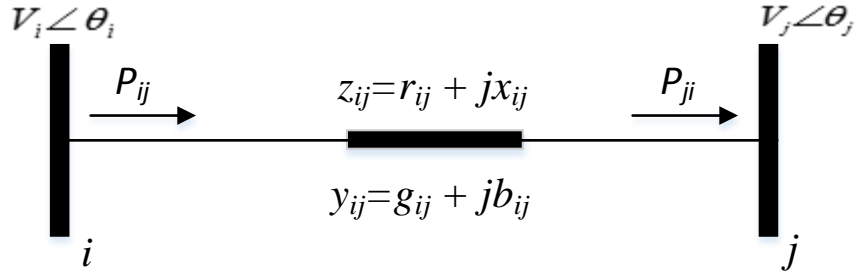
Figure 2.1 Model of a transmission line connecting bus i and bus j

Upon simplification,

$$P_{ij} = g_{ij}\left[V_i^2 - V_i \cdot V_j \cdot \cos(\theta_i - \theta_j)\right] - b_{ij} \cdot V_i \cdot V_j \cdot \sin(\theta_i - \theta_j) \qquad (2.2)$$

Similarly,

$$P_{ji} = -g_{ij}\left[V_j^2 - V_i \cdot V_j \cdot \cos(\theta_i - \theta_j)\right] - b_{ij} \cdot V_i \cdot V_j \cdot \sin(\theta_i - \theta_j) \qquad (2.3)$$

Where,

V_i = voltage at bus i in per unit

Vj = voltage at bus i in per unit

θ_i = angle at bus i

θ_j = angle at bus j

r_{ij} = resistance of transmission line i-j in per unit

x_{ij} = reactance of transmission line i-j in per unit

z_{ij} = impedance of transmission line i-j in per unit

y_{ij} = admittance of transmission line i-j in per unit

g_{ij} = conductance of transmission line i-j in per unit

b_{ij} = susceptance of transmission line i-j in per unit

P_{ij} = Power flow from bus i to bus j in per unit

P_{ji} = Power flow from bus j to bus i in per unit

It can be seen that the difference of the flows at the sending and receiving ends of the branch represent losses that occur on the branch.

Occasionally, phase shifting transformers are found in the large networks to regulate the real power flow over the transmission lines. Therefore, a generalized model for phase shifting transformer involving taps is derived.
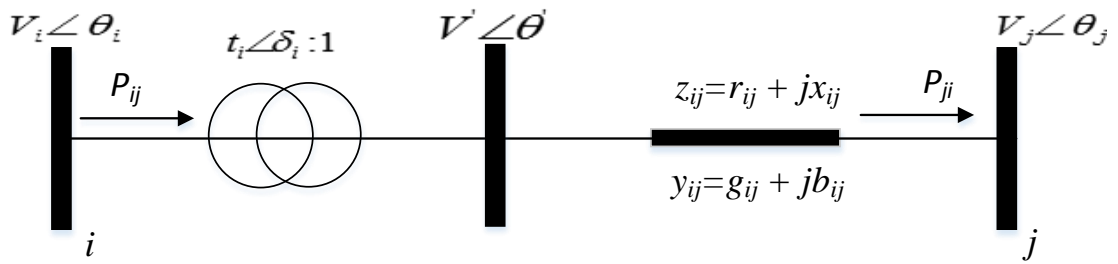
Figure 2.2 Model of a phase shifting transformer connecting bus i and j

Figure 2.2 shows a phase shifting transformer connecting buses i and j. A fictitious bus is added for clarity to separate the transformer impedance from transformation ratio. It is to be noted that the phase-shift transformer makes the bus admittance matrix Y_{bus} asymmetric. Power flow at the sending end is obtained as follows [31] – [33]:

$$P_{ij} = \text{Re}\left\{ \frac{V_i \angle \theta}{t_i \angle \delta_i} \cdot \left[\left(\frac{V_i \angle \theta}{t_i \angle \delta_i} - V_j \angle \theta_j \right) \cdot (g_{ij} + j \cdot b_{ij}) \right]^* \right\}$$

$$P_{ij} = g_{ij}\left[\frac{V_i^2}{t_i^2} - \frac{V_i \cdot V_j}{t_i} \cdot \cos(\theta_i - \theta_j - \delta_i) \right] - b_{ij} \cdot \frac{V_i \cdot V_j}{t_i} \cdot \sin(\theta_i - \theta_j - \delta_i)$$

(2.4)

Similarly, the receiving end power flow is given as:

$$P_{ji} = -g_{ij}\left[V_j^2 - \frac{V_i \cdot V_j}{t_i} \cdot \cos(\theta_i - \theta_j - \delta_i) \right] - b_{ij} \cdot \frac{V_i \cdot V_j}{t_i} \cdot \sin(\theta_i - \theta_j - \delta_i)$$

(2.5)

where,

t_i = tap ratio of the transformer.

δ_i = phase shift angle of the transformer

2.2 CLASSICAL DC POWER FLOW MODEL DERIVATION

To derive the classical dc power-flow model, the classical assumptions are applied to the ac branch flow model without the phase shifting transformer. The following assumptions are made for the dc power-flow model:

Assumption 1: Losses are neglected on the branch i.e. resistance is neglected.

$r \approx 0 \rightarrow g_{ij} = 0$ *and* $b_{ij} = -1/x_{ij}$;

Assumption 2: Voltage at the buses are approximate to 1 p.u.

$V_i \approx 1$ for all bus *i;*

Assumption 3: The angle difference across the branch end is small such that

$\sin(\theta_{ij}) \approx \theta_{ij}$

Assumption 4: Transformer taps are ignored as voltage is 1 per unit at each bus.

$t_i \qquad \approx 1$

The introduction of these assumptions in the ac power flow model introduces errors which shall be discussed later in this chapter. These assumptions modify the active power flow equations for bus *i* and bus *j* derived in (2.4) - (2.5) as follows:

$$P_{ij} = P_{ji} = -b_{ij} \cdot (\theta_i - \theta_j) \qquad\qquad (2.6)$$
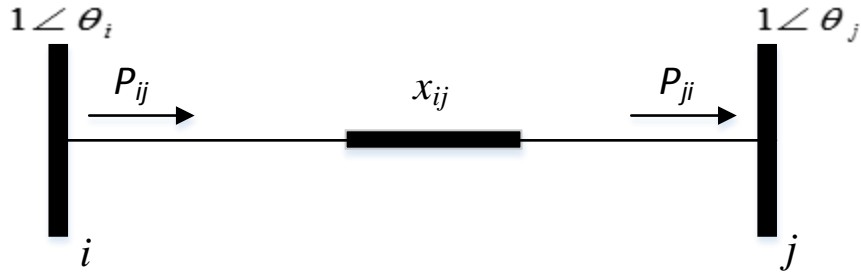
Figure 2.3 Typical dc model of a transmission line connecting bus *i* and *j*

The node balance equation for an N+1 bus system (one bus is slack or reference bus) and L branch network using (2.6) yields the generalized equation for dc power flow model as:

$$P_{inj} = B_{bus} \cdot \theta \tag{2.7}$$

where,

$$P_{inj}^i = \sum_{i=1}^{N} (P_G^i - P_L^i) \qquad = \text{N} \times 1 \text{ bus injection vector} \quad \forall \ \text{i} \in 1, 2...\text{N}$$

P_G^i = Power generated at bus *i*

P_L^i = Load at bus *i*

B_{bus} = C^T. *diag(1/x)* . *C*   = N × N bus susceptance matrix

Θ = Bus voltage angles

C   = L × N bus-branch incidence matrix

(1/x)   = [*1/x₁, 1/x₂, 1/x₃.....1/xₗ*]   = susceptance of the network model

diag(1/x) = L × L diagonal matrix containing network susceptance

Also, the generalized equation for the power flow over the network branches can be written as:

$$P_{flow} = B_{branch} \cdot \theta \qquad\qquad (2.8)$$

where

P_{flow} $= L \times 1$ network branch power flow vector

$B_{branch} = diag(1/x) \cdot C$ $= L \times N$ branch susceptance matrix

The solution involves solving the linear system of equations, (2.7), from which nodal

phase angles are obtained using sparse LU factorization of B_{bus} and then performing

forward/backward substitution. Power flow over the network branch is obtained using

(2.8).

As mentioned earlier, phase shifters alter the real power flow over the transmission

line. Therefore, its implications on the dc power flow equations must be accounted for.

The power flow over a branch with phase shifter is given by:

$$P_{ij} = P_{ji} = -b_{ij} \cdot (\theta_i - \theta_j - \delta_i) \qquad\qquad (2.9)$$

Using node balance equations, the dc bus injection and branch flow equations are

modified as:

$$P_{inj} = B_{bus} \cdot \theta + P_{bus}^{shift}$$
$$\qquad\qquad (2.10)$$
$$P_{flow} = B_{branch} \cdot \theta + P_{branch}^{shift}$$

where, P_{bus}^{shift} and P_{branch}^{shift} represent the power injection vectors that compensate for the

phase shifter on both the bus power injection and branch flow equation.

2.3   ERRORS DUE TO DC POWER FLOW ASSUMPTIONS

Although, the objective of this research is not to analyze in detail either the impacts of assumptions used in dc model creation or the impacts of loading on such a model, it is desirable to have a comprehensive view of these dc-modeling assumptions.

Assumption #1 above states that the losses are neglected. At first glance, it implies that this assumption results in an error of few percent over the network branch. However, these small errors over all the lines accumulate and appear on the slack or reference bus. Therefore, for a large power system the power flows over the transmission lines in the vicinity of this reference bus results in large errors. This effect will be observed in the ERCOT interconnection model discussed later in this report when the comparison of ac and dc power flows will be made at the base case and under contingency.

The second assumption above states that the bus voltages are assumed to be 1 per unit. This assumption directly implies the absence of transformer taps and the absence of line voltage drop. It is typical of the NERC-MMWG models to have voltages in the range of 0.75 to 1.4 per unit. Therefore the real power-flow error due to this assumption is in the range -43.75% to 96%. This assumption impacts the VAR flow over the line and hence the effective value of current, therefore, large deviations from this assumption in conjunction with the loss neglecting assumption (i.e. R=0) can lead to large errors in the dc power flows obtained from such a model.

The third assumption above states that the angle difference across a transmission line is small which approximates $\sin(\theta) \approx \theta$. This assumption is typically accurate for short transmission lines. However, for a longer transmission lines, the angle across the line may be larger. This may result in introducing significant error. For example a 40° angle across the transmission line introduces an error of 8.6% due to this assumption.

It may seem from the above discussion that these assumptions lead to inaccurate power flow results by a large margin. However, in practice this *may* not hold true. Consider the following argument. First recognized that the dc network model is just a linear direct–current divider circuit model. Therefore, it follows that MW flows are divided according to Ohm's and Kirchoff's law where real power flows are analogous to current and bus angles are analogous to voltages. For example, if all the bus voltages are identical but not equal to 1 per unit, then the assumption of 1 per unit bus voltages will have no impact on the error of the dc power flow model. As another example, when there is a radial line no errors are induced apart from losses due to the assumption numbers one and three stated above. It often becomes difficult to predict if the assumptions made will accumulate errors or display self-cancellation properties or propagate the MW flow inaccuracies throughout dc network when power flows are obtained from such a model. For more details, an interested reader should look at [9]-[10] which discuss the impact of such assumption on realistic power systems.

2.4 GENERALIZED DC POWER FLOW MODEL

The dc model discussed so far is a lossless model involving only series elements i.e. reactance or susceptance, therefore there is no provision of any loss compensation. In this section a more generalized dc power flow model is formulated.
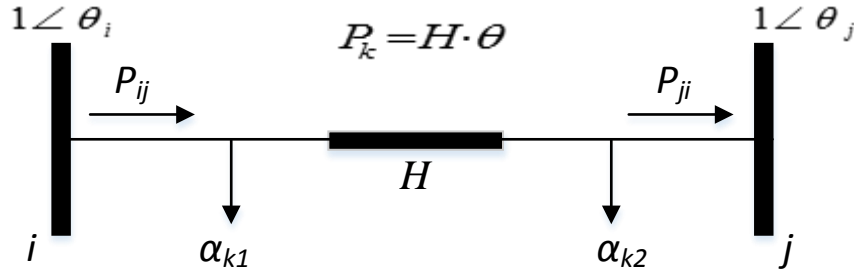
Figure 2.4 A generalized dc model of a branch connecting bus *i* and *j*

The generalized dc power flow model for a transmission shown in Figure 2.4 [6], indicates a series element i.e. reactance or susceptance represented by *H*. The flow over the branch is given by:

$$P_k = H \cdot \theta \qquad\qquad (2.11)$$

where

P_k = Power flow over the transmission line

H = Susceptance of the branch

$\theta = \theta_i - \theta_j$ = Angle difference across the branch

α_{k1} = Sending end loss compensation for branch

α_{k2} = Receiving end loss compensation for branch

This model incorporates losses (based on the solved ac solution) that occur over the entire network by modeling the (negative) power injections at the respective buses. It is

worthwhile to note that sum of $\alpha_{k1} + \alpha_{k2}$ represent the total loss that appears over the branch due any resistive element in the ac model.

Various dc power flow models are now introduced with respect to this generalized dc power flow model.

2.4.1   COLD START OR STATE INDEPENDENT DC MODEL

Cold start dc models a.k.a. state independent models are a common type of dc model used when there is an absence of reliable solved ac base case solution. Therefore, these type of dc models do not account for the losses that occur over the system, i.e. there is no loss compensation. Due to the absence of loss modeling, this model often leads to a less accurate power flow solution. However, this type of dc model is quite prevalent in industry and extensively used for SCUC, FTR and long term planning purposes.

Mathematically, it is defined as:

$$H = \frac{1}{x_{ij}}$$

(2.12)

$\alpha_{k1} = \alpha_{k2} = 0$ (No loss compensation)

The power flow solution using this model is obtained as explained in section 2.2.

Another suggested approach to cold start models, where there is lack of good voltage/VAR solution, is to use a fixed-voltage ac power-flow solution. In this model, bus voltages and transformer taps are set to 1 per unit i.e. all buses are specified as PV

buses with no VAr limit. Although the VAr flows obtained from such a flat voltage ac

solution are completely wrong, the MW flows, net losses or loss distribution obtained

from such an approach is better than the no-loss or classical dc model.

2.4.2   HOT START OR STATE DEPENDENT DC MODEL

In this type of dc model, series and shunt elements are developed based on the

solved ac network solution and remain fixed thereafter. Therefore, for a given network

topology *a priori* knowledge of the losses is obtained and incorporated as injections or

withdrawals at the buses; therefore, the load generation balance in this model is similar

to the full blown ac model, i.e. losses match exactly those of the ac model. These types

of models are used in SCED using a state estimator solution [6] and short/medium term

operations/planning studies.

In this section, two common hot start dc models shall be discussed.

2.4.2.1   Single multiplier or Net loss dispersal dc model

This type of dc model is similar to the classical dc model described above.

However, the total losses are distributed across the network by scaling all the loads

using a constant multiplier γ. This constant multiplier γ is defined as a ratio of total

generation (load + losses) to total load in the network. The single multiplier is defined

mathematically as:

$$\gamma = \frac{\sum\limits_{i=1}^{N} P_G^i}{\sum\limits_{i=1}^{N} P_L^i} \qquad\qquad (2.13)$$

Other variations for this dc model involve the use of zonal multipliers. Zonal multipliers are obtained in a similar fashion to single multiplier. In this case, loads in respective zones are scaled up by their zonal multipliers obtained using the load generation balance in respective zones.

Parameters corresponding to a generalized model for the single multiplier type loss compensation is given as:

$$H = \frac{1}{x_{ij}} \qquad\qquad (2.14)$$

$$\alpha_i = (\gamma - 1) \cdot P_L^i \qquad \forall i \in 1,2,\cdots,N \quad nodes$$

2.4.2.2 Base point matching or Alpha-matching dc model

This model introduces localized loss compensation at the buses connected to the transmission line. This model matches the MW flows and nodal phase angles obtained from the ac power flow solution perfectly [6]. In this model, the H parameter is specified beforehand and the corresponding loss compensation injections (α's) are then calculated based on solved ac power flow. Although, the detailed derivation to obtain optimized series element H parameter shall be dealt with in the next chapter, the mathematical relations for all the model parameters is given as follows:

19

$$H = \frac{1}{x_{derived}}$$

$$\alpha_{k1} = P_{ij}^o - H \cdot (\theta_i^o - \theta_j^o) \tag{2.15}$$

$$\alpha_{k2} = -P_{ji}^o + H \cdot (\theta_i^o - \theta_j^o)$$

where

^{o} superscript denotes the values obtained from the ac base case solution.

In comparison to all other dc models discussed so far, this model best fits itself to the solved ac solution and can predict the small perturbation around the operating point.

The discussion on dc power flow models is incomplete without introducing reader to the nonlinearities associated with the continuous acting control devices like phase–shifters, tap changers, HVDC, FACTS devices, active during the "outer loop" of the ac power flow. For example, the phase-shifter angle will vary within a prescribed range to control the power flow while it will act as fixed-angle transformation when the lower/upper limit is hit. This leads to discontinuities in the system model and may lead to inaccurate MW flows over the lines if modeling is not handled properly. If necessary such nonlinearities can be accounted for by using iterative procedures but then some of the advantage of using dc model is eliminated as it becomes more computationally complex.

The discussion of the dc power model can be summarized by stating that these models provide qualitative insight into the system, however, the accuracy of these models varies over networks with loading conditions. Due to pervasive use of such

models in market applications, the accuracy of dc models is of great interest especially

when the critical paths are under consideration.

3 PTDF BASED DC SERIES ELEMENT MODEL

3.1 INTRODUCTION

A dc model is made up of two distinct element types, series and shunt, and the methods used to get values for each element type may be, and often are, handled independently. The lossless series element has units of susceptance and is used to approximate the power-flow angle-difference relationship of a network branch. The dc series elements act similar to a current divider network and these elements divide the power across the network branches in accordance with Ohm's law. The shunt element has units of power and models the effect of losses in some fashion.

The focus of this chapter is the development of an optimized dc series element model for the base point matching or alpha-matching dc model introduced in the previous chapter. First, the mathematical inter-relationship of power transfer distribution factor (PTDF) and reactance shall be derived. Second, the problems associated with ac PTDFs shall be considered and their conversion to equivalent dc PTDFs is discussed. Finally, an optimization problem is then formulated to derive the equivalent dc model from these derived dc PTDFs.

3.2 GENERAL DC SERIES ELEMENT MODEL

The dc power flow formulation for an N+1 buses (N – non-reference bus and 1 reference/slack bus) and L branches model is represented by (2.7) and (2.8) matrix equations repeated below:

$$P_{inj} = B_{bus} \cdot \theta \tag{3.1}$$

$$P_{flow} = B_{branch} \cdot \theta \tag{3.2}$$

On substituting (3.1) in (3.2),

$$P_{flow} = B_{branch} \cdot B_{bus}^{-1} \cdot P_{inj} \tag{3.3}$$

Therefore,

$$P_{flow} = \phi \cdot P_{inj} \tag{3.4}$$

where,

$$\phi = B_{branch} \cdot B_{bus}^{-1} \tag{3.5}$$

$$= L \times N \text{ PTDF matrix or sensitivity factor matrix.}$$

This gives the relationship of PTDF matrix to the power flow over network branches and bus injections at respective buses.

3.3 POWER TRANSFER DISTRIBUTION FACTORS (PTDFs)

A power transfer distribution factor is defined as the linear sensitivity of line flow to the injection at particular bus and withdrawal at sink bus. If the amount of power Δt is injected at bus k (injection bus) and same amount of power is withdrawn from bus $N+1$ (sink bus) [34], we define the PTDF for the line connecting bus i and bus j as:

$$\phi_{ij_k}^{N+1} = \frac{\Delta P_{ij}}{\Delta t} \tag{3.6}$$

where,

ΔP_{ij} = change in power flow over branch ij

$\phi_{ij_k}^{N+1}$ = PTDF for branch ij due to injection at bus i and withdrawal at slack bus

Δt = Power transacted between bus i and bus $N+1$ *(slack/reference bus)*
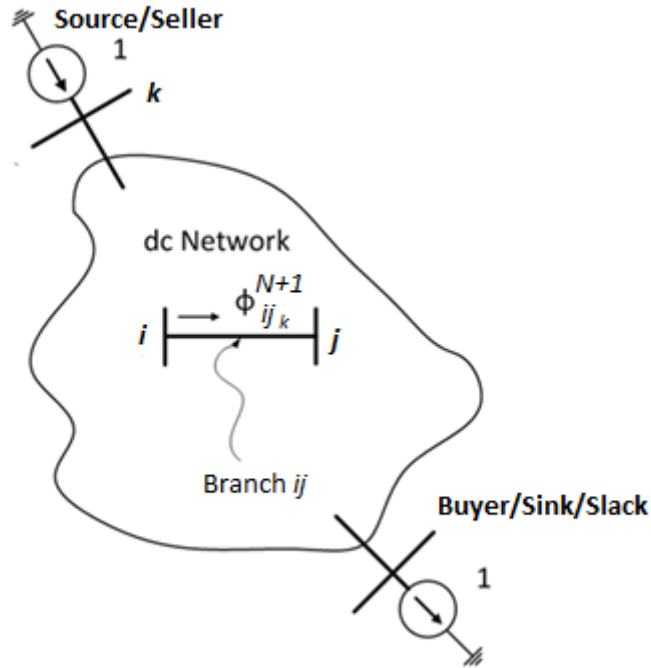
Figure 3.1 dc network representing PTDF for branch *ij*

In the similar fashion, a matrix corresponding to the transaction between the each bus to reference bus is constructed, this is known as the PTDF (ϕ) matrix in (3.5) and the column corresponding to each injection bus is defined as injection shift factor (Ψ). The PTDFs obtained are functions of network branch parameters (i.e. reactance) and network topology. Any change to these parameters typically leads to a change in these sensitivity factors.

However, the PTDF matrix obtained in (3.5) is based on the classical dc model and its assumptions. These classical dc PTDFs have unpredictable accuracy and can lead to

large errors in estimating flow sensitivities when the network deviates from the nominal conditions, like 1 per unit bus voltage, or has branches with low X/R ratios or large angle difference across the line; in contrast the ac PTDFs do take into account such sensitivities that arise due to network topology, branch parameters and network operating point. Therefore, ac PTDFs can provide a better allocation of MW's across the network than the classical dc PTDFs and can be used to obtain a better network dc equivalent model for market application and planning studies.

3.3.1   Classical DC PTDF derivation

In furtherance of the state goal of this research, it is beneficial to recognize that the bus susceptance matrix (B_{bus}) and branch susceptance matrix (B_{branch}) can be written in terms of the bus-branch incidence matrix (C) and network reactance (x) as follows:

$$B_{bus} = C^T \cdot diag\left(\frac{1}{x}\right) \cdot C \tag{3.7}$$

$$B_{branch} = diag\left(\frac{1}{x}\right) \cdot C \tag{3.8}$$

where,

C $= L \times N$ Bus-branch incidence matrix

C^T $=$ Transpose of bus-branch incidence matrix

$$diag\left(\frac{1}{x}\right) = \begin{bmatrix} 1/x_1 & 0 & 0 & 0 \\ 0 & 1/x_2 & 0 & 0 \\ 0 & 0 & \ddots & 0 \\ 0 & 0 & 0 & 1/x_L \end{bmatrix}_{L \times L} \text{and} \quad x = \begin{bmatrix} x_1 \\ x_2 \\ \vdots \\ x_L \end{bmatrix}$$

On substituting (3.7) and (3.8) into (3.5), dc PTDFs as a function of network parameter

and topology are obtained as:

$$\phi = diag\left(\frac{1}{x}\right) \cdot C \cdot \left[C^T \cdot diag\left(\frac{1}{x}\right) \cdot C\right]^{-1} \tag{3.9}$$

Since these PTDFs are derived from an ideal lossless model, ϕ is said to be consistent

in the following three ways:

- The PTDFs at the sending and receiving end are exactly same
- PTDFs are consistent along the injection shift factor i.e. sum of injections at the non-source buses is zero.
- PTDFs are consistent across the injection shift factors i.e. there exist a unique (can be uniformly scaled values though) set of reactance that can satisfy all the injection shift factors simultaneously.

3.3.2 Linearized AC PTDFs derivation

The incremental ac PTDFs are defined by linearizing the ac power flow equations

obtained for branch ij ((2.1)– (2.5)) around the base operating point. Mathematically,

these ac PTDFs are defined as:

$$\phi_{ij_k}^{N+1} = \left.\frac{\Delta P_{ij}}{\Delta t}\right|_{\theta=\theta_o, V=V_o} \tag{3.10}$$

where,

∂P_{ij} = Incremental change in power flow over branch ij due to injection at bus k

θ_o = Angle from solved ac base case solution

V_o = Voltage magnitude from solved ac base case solution
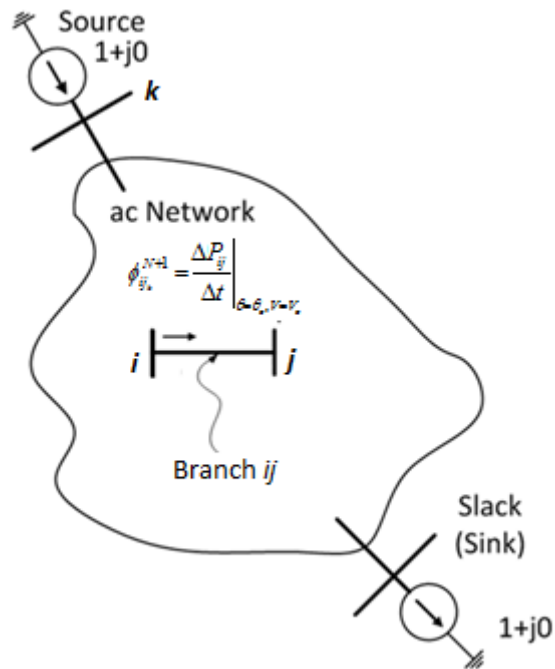
Figure 3.2 ac network representing ac PTDF for branch *ij*

Alternatively, these sensitivities can be obtained from the final Jacobian formed in the Newton-Raphson method based ac power flow. Since the approach involves evaluating the Jacobian it makes sense to discuss the basic ac power flow equations [35] at this point.

3.3.2.1   The ac power flow equations.

For the typical transmission line model shown in Figure 2.1, the power balance equations for bus *i* are defined as:

For PQ bus (or for PV bus on VAr limits)

$$P_i = V_i \sum_j \left[V_j \left(g_{ij} \cos(\theta_i - \theta_j) + b_{ij} \sin(\theta_i - \theta_j) \right) \right] \tag{3.11}$$

$$Q_i = V_i \sum_j \left[V_j \left(g_{ij} \cos(\theta_i - \theta_j) - b_{ij} \sin(\theta_i - \theta_j) \right) \right] \tag{3.12}$$

For PV bus (within VAr limits)

$$P_i = V_i \sum_j \left[V_j \left(g_{ij} \cos(\theta_i - \theta_j) + b_{ij} \sin(\theta_i - \theta_j) \right) \right] \tag{3.13}$$

$$V_i = V_i^{sp} \tag{3.14}$$

where,

P_i = net real power injection to bus i = $P_G^i - P_L^i$

Q_i = net reactive power injection to bus i = $Q_G^i - Q_L^i$

P_G^i = net real power injection at bus i due to generators

Q_G^i = net reactive power injection at bus i due to generators

P_L^i = net real power withdrawn at bus i due to loads

Q_L^i = net reactive power withdrawn at bus i due to loads

V_i^{sp} = specified voltage at bus i if it is a PV bus

The incremental values of the unknown system variables, i.e. V and θ, are given by:

$$\begin{bmatrix} \Delta P \\ \Delta Q \end{bmatrix} = \begin{bmatrix} J1 & J2 \\ J3 & J4 \end{bmatrix} \cdot \begin{bmatrix} \Delta \theta \\ \Delta V \end{bmatrix} \tag{3.15}$$

where,

$\begin{bmatrix} J1 & J2 \\ J3 & J4 \end{bmatrix}_{(2N-m) \times (2N-m)}$ = Jacobian matrix; m = number of PV buses

$$\begin{bmatrix} \Delta P \\ \Delta Q \end{bmatrix}_{(2N-m)\times 1} \quad = \text{represents real and reactive power mismatch}$$

$$\begin{bmatrix} \Delta \theta \\ \Delta V \end{bmatrix}_{(2N-m)\times 1} \quad = \text{incremental bus angle and voltage magnitude}$$

$\forall i \neq j$

$$J1 = \frac{\partial P_i}{\partial \theta_j} = V_i \cdot V_j \left[g_{ij} \sin(\theta_i - \theta_j) - b_{ij} \cos(\theta_i - \theta_j) \right]$$

$$J2 = \frac{\partial P_i}{\partial V_j} = V_i \cdot \left[g_{ij} \sin(\theta_i - \theta_j) + b_{ij} \cos(\theta_i - \theta_j) \right]$$

$$J3 = \frac{\partial Q_i}{\partial \theta_j} = -V_i \cdot V_j \left[g_{ij} \cos(\theta_i - \theta_j) + b_{ij} \sin(\theta_i - \theta_j) \right]$$

$$J4 = \frac{\partial Q_i}{\partial V_j} = V_i \cdot \left[g_{ij} \sin(\theta_i - \theta_j) - b_{ij} \cos(\theta_i - \theta_j) \right]$$

$$(3.16)$$

$\forall i = j$

$$J1 = \frac{\partial P_i}{\partial \theta_i} = -Q_i^{calc} - B_{ii} V_i^2$$

$$J2 = \frac{\partial P_i}{\partial V_i} = -\frac{P_i^{calc}}{V_i} + G_{ii} V_i$$

$$J3 = \frac{\partial Q_i}{\partial \theta_i} = P_i^{calc} - G_{ii} V_i^2$$

$$J4 = \frac{\partial Q_i}{\partial V_i} = \frac{Q_i^{calc}}{V_i} - B_i V_i$$

where,

$$P_i^{calc} = V_i \sum_j \left[V_j \left(g_{ij} \cos(\theta_i - \theta_j) + b_{ij} \sin(\theta_i - \theta_j) \right) \right]$$

$$Q_i^{calc} = V_i \sum_j \left[V_j \left(g_{ij} \sin(\theta_i - \theta_j) - b_{ij} \cos(\theta_i - \theta_j) \right) \right]$$

The Jacobian matrix in (3.15) is a sparse matrix. Solution of (3.15) is obtained using sparse LU factorization [35]-[36] of this matrix and then sparse forward/backward substitution.

3.3.2.2 Sensitivity calculation for bus voltage magnitude and angle

As stated earlier, the Jacobian matrix provides the sensitivity of power injections to both bus voltage magnitudes and angles. Conversely, for an incremental power injection at a particular bus, (3.15) provides the bus voltage magnitude and angle sensitivities. Using these bus voltage magnitude and angle sensitivities, one can obtain the MW flow sensitivities; hence one can obtain the MW flow sensitivity due to the incremental injection at a given bus which is the definition of ac PTDF given in (3.10).

Define the $N+1^{th}$ bus as the slack bus/sink bus and let the kth bus be the injection bus. Let $\Delta P_{transacted}$ of dimension $N \times 1$ be the real power transaction vector between the source and the sink bus. Similarly $\Delta Q_{transacted}$ be of cardinality $N \times 1$ and represent the reactive power transaction vector. Since the PTDFs are defined for MW flow sensitivity to incremental MW injection at bus, the mathematical formulation [37] for these sensitivities is obtained as:

- $\Delta P^k_{transacted}$ contains only 0's and 1's.

- $\Delta P^k_{transacted}$ is 1 at the kth position corresponding to the injection bus k and the remaining elements of vector are 0 value corresponding to the non-injection bus.

- $\Delta Q^k_{transacted}$ is 0 value for all its element, as reactive power is not of interest at this stage.

30

$$\downarrow k^{th}\ element \qquad (3.17)$$

$$\Delta P^k_{transacted} = [0,0,\cdots,0,1,0\cdots,0]^T$$
$$\Delta Q^k_{transacted} = [0,0,\cdots,0,0,0\cdots,0]^T \qquad (3.18)$$

Thus, (3.17) and (3.18) can now be substituted in (3.15) to obtain the bus voltage

magnitude and angle sensitivity for injection at k^{th} bus as:

$$\begin{bmatrix} \Delta P^k_{transacted} \\ \Delta Q^k_{transacted} \end{bmatrix} = \begin{bmatrix} J1 & J2 \\ J3 & J4 \end{bmatrix} \cdot \begin{bmatrix} \Delta \theta^k \\ \Delta V^k \end{bmatrix} \qquad (3.19)$$

Upon simplification,

$$\begin{bmatrix} \Delta \theta^k \\ \Delta V^k \end{bmatrix} = \begin{bmatrix} J1 & J2 \\ J3 & J4 \end{bmatrix}^{-1} \cdot \begin{bmatrix} \Delta P^k_{transacted} \\ \Delta Q^k_{transacted} \end{bmatrix} \qquad (3.20)$$

This process is repeated by considering each injection bus, one at a time, and the

corresponding bus voltage magnitude and angle sensitivities are calculated.

Alternatively, it can be seen that each column vector obtained from the inverse of the

Jacobian matrix provides the bus voltage magnitude and angle sensitivities

corresponding to the each injection bus k.

3.3.2.3   ac PTDF/Branch MW flow sensitivity calculation

Recall the ac power flow equations (2.1)-(2.3) representing the power flow over

branch ij (refer to Figure 2.1), which can be re-written as:

$$P_{ij} = g_{ij}\left[V_i^2 - V_i \cdot V_j \cdot \cos(\theta_i - \theta_j)\right] - b_{ij} \cdot V_i \cdot V_j \cdot \sin(\theta_i - \theta_j)$$

$$P_{ji} = -g_{ij}\left[V_j^2 - V_i \cdot V_j \cdot \cos(\theta_i - \theta_j)\right] - b_{ij} \cdot V_i \cdot V_j \cdot \sin(\theta_i - \theta_j)$$

31

$$Q_{ij} = -g_{ij}V_i \cdot V_j \cdot \sin(\theta_i - \theta_j) - b_{ij}\left[V_i^2 - V_i \cdot V_j \cdot \cos(\theta_i - \theta_j)\right]$$

$$Q_{ji} = -g_{ij}V_i \cdot V_j \cdot \sin(\theta_i - \theta_j) + b_{ij}\left[V_j^2 - V_i \cdot V_j \cdot \cos(\theta_i - \theta_j)\right]$$

The MW flow sensitivity for a branch *ij* can be obtained by considering the partial differential equation of power flow to bus voltage magnitude and angle as:

$$\Delta P_{ij} = \frac{\partial P_{ij}}{\partial \theta_i} \cdot \Delta\theta_i + \frac{\partial P_{ij}}{\partial \theta_j} \cdot \Delta\theta_j + \frac{\partial P_{ij}}{\partial V_i} \cdot \Delta V_i + \frac{\partial P_{ij}}{\partial V_j} \cdot \Delta V_j \tag{3.21}$$

$$\Delta Q_{ij} = \frac{\partial Q_{ij}}{\partial \theta_i} \cdot \Delta\theta_i + \frac{\partial Q_{ij}}{\partial \theta_j} \cdot \Delta\theta_j + \frac{\partial Q_{ij}}{\partial V_i} \cdot \Delta V_i + \frac{\partial Q_{ij}}{\partial V_j} \cdot \Delta V_j \tag{3.22}$$

where,

$$\frac{\partial P_{ij}}{\partial \theta_i} = V_i \cdot V_j \cdot g_{ij} \cdot \sin(\theta_i - \theta_j) - V_i \cdot V_j \cdot b_{ij} \cdot \cos(\theta_i - \theta_j)$$

$$\frac{\partial P_{ij}}{\partial \theta_j} = -V_i \cdot V_j \cdot g_{ij} \cdot \sin(\theta_i - \theta_j) + V_i \cdot V_j \cdot b_{ij} \cdot \cos(\theta_i - \theta_j)$$

$$\frac{\partial P_{ij}}{\partial V_i} = g_{ij}\left[2V_i - V_j \cos(\theta_i - \theta_j)\right] - b_{ij} \cdot V_j \cdot \sin(\theta_i - \theta_j) \tag{3.23}$$

$$\frac{\partial P_{ij}}{\partial V_j} = -g_{ij} \cdot V_i \cdot \cos(\theta_i - \theta_j) - b_{ij} \cdot V_i \cdot \sin(\theta_i - \theta_j)$$

$$\frac{\partial Q_{ij}}{\partial \theta_i} = -V_i \cdot V_j \cdot g_{ij} \cdot \sin(\theta_i - \theta_j) - V_i \cdot V_j \cdot b_{ij} \cdot \cos(\theta_i - \theta_j)$$

$$\frac{\partial Q_{ij}}{\partial \theta_j} = V_i \cdot V_j \cdot g_{ij} \cdot \sin(\theta_i - \theta_j) + V_i \cdot V_j \cdot b_{ij} \cdot \cos(\theta_i - \theta_j)$$

$$\frac{\partial Q_{ij}}{\partial V_i} = g_{ij} \cdot V_j \cos(\theta_i - \theta_j) - b_{ij} \cdot V_j \cdot \sin(\theta_i - \theta_j) - 2 \cdot V_i \cdot b_{ij} \tag{3.24}$$

$$\frac{\partial Q_{ij}}{\partial V_j} = g_{ij} \cdot V_i \cos(\theta_i - \theta_j) - b_{ij} \cdot V_i \cdot \sin(\theta_i - \theta_j)$$

The variables $\Delta\theta$ and ΔV used in (3.21) are obtained by solving (3.19). And finally the ac PTDFs are calculated using (3.10), (3.21). and $\Delta t = 1$ MW (incremental injection

at bus k). Δt represents the power transacted between the source (k^{th} bus in (3.17)) and

sink bus.

The ac PTDF matrix thus obtained is inconsistent if used as a dc PTDF matrix in all

respects mentioned earlier as it accounts for the nonlinearities like losses, in the model.

This matrix is accompanied with following inconsistencies:

- The PTDFs at the sending and receiving end are not same.
- PTDFs are inconsistent along the injection shift factor i.e. sum of injections at the non-source buses is zero.
- PTDFs are inconsistent across the injection shift factors i.e. there does not exist a unique set of reactance that can satisfy all the injection shift factors simultaneously.

3.4 PTDF-BASED OPTIMIZATION APPROACHES

Relatively recently, bus aggregation techniques (as opposed to bus elimination

techniques such as Ward reduction) have been introduced as an alternative for creating

reduced network equivalents that perform better in some applications [15]-[17]. Bus

aggregation techniques are PTDF-based and rely on solving an optimization problem to

find the network series elements of a reduced network, given the PTDF matrix of the

network under study. In essence, these methods take a large consistent PTDF matrix

and find a smaller "equivalent" PTDF matrix from which the series elements of a

reduced network can be inferred. This approach can be used to advantage in the work

here by applying it with the following change: We take a large inconsistent PTDF

matrix and, in essence, map it to a partially consistent PTDF matrix of the same size and sparsity pattern, from which we infer the series elements of the dc network model.

Typically we have topology and the branch susceptance from which we calculate the dc PTDF matrix, ϕ. Our situation is a bit different. We have an ac PTDF matrix (from which we will calculate a dc PTDF matrix) and wish to find the branch reactances consistent with this dc PTDF matrix. This can be accomplished in the following way.

Equation (3.9) may be manipulated as follows,

$$\phi \cdot \left[C^T \cdot diag\left(\frac{1}{x}\right) \cdot C \right] = diag\left(\frac{1}{x}\right) \cdot C \tag{3.25}$$

$$\phi \cdot \left[C^T \cdot diag\left(\frac{1}{x}\right) \cdot C \right] - diag\left(\frac{1}{x}\right) \cdot C = 0 \tag{3.26}$$

$$\left[\phi \cdot C^T - I\right] \cdot diag\left(\frac{1}{x}\right) \cdot C = 0 \tag{3.27}$$

Using the matrix algebra for further simplification,

$$\left[\phi \cdot C^T - I\right] \cdot diag(c_m) \cdot \left[\frac{1}{x}\right] = 0, \qquad m = 1, 2, \ldots, N \tag{3.28}$$

where,

    C = Bus-branch incidence matrix = $[c_1, c_2..., c_m, ...c_N]$

    c_m = m^{th} column vector of bus-branch incidence matrix

$diag(c_m)$ = diagonal matrix formed using c_m

Alternatively,

$$\Lambda \cdot \left[\frac{1}{x} \right] = 0 \tag{3.29}$$

where,

$$\Lambda = \begin{bmatrix} (\phi \cdot C^T - I) \cdot diag(c_1) \\ (\phi \cdot C^T - I) \cdot diag(c_2) \\ \ldots\ldots\ldots\ldots\ldots\ldots \\ (\phi \cdot C^T - I) \cdot diag(c_N) \end{bmatrix}_{N \cdot L \times L} \tag{3.30}$$

Several observations about this over-determined set of equations, (3.29), are important. First, the trivial solution to (3.29), ($1/x = 0$) is of no interest. This implies that all line reactances are infinite, i.e., all branches are open circuited. Equation (3.29) and (3.30) describe Λ-matrix which has a rank of at most L-1, and is therefore rank deficient. Because the dc power-flow problem is based on linear angle-flow relationships and linear bus-power-balance constraints, it can be thought of as a "current divider" network where current is the analog of power. Since the series branch values of any dc network with only series branch "resistances" and shunt current injections can be scaled by an arbitrary constant without affecting the "current division" properties, (3.29) should be rank deficient by at least one degree.

3.5   CONVERSION FROM AC PTDFs TO DC PTDFs

Rank-deficiency notwithstanding, a unique solution to (3.29) exists with all residuals identically equal to zero if the (dc) PDTF matrix is consistent. More precisely, the PTDF matrix consistency and inconsistency can be stated as: each column, or injection shift factor, is self-consistent if a network model could be created which corresponds

exactly to the injection shift factor. If all columns, or injection shift factors, are mutually

consistent (i.e., the PTDF matrix is fully consistent) then a network model could be

created which corresponds exactly to all injection shift factors simultaneously. The ac

PTDF matrix is consistent in neither of these ways because of the branch power losses.

A method for creating a partially consistent dc PTDF matrix from an inconsistent ac

PTDF matrix is introduced next.
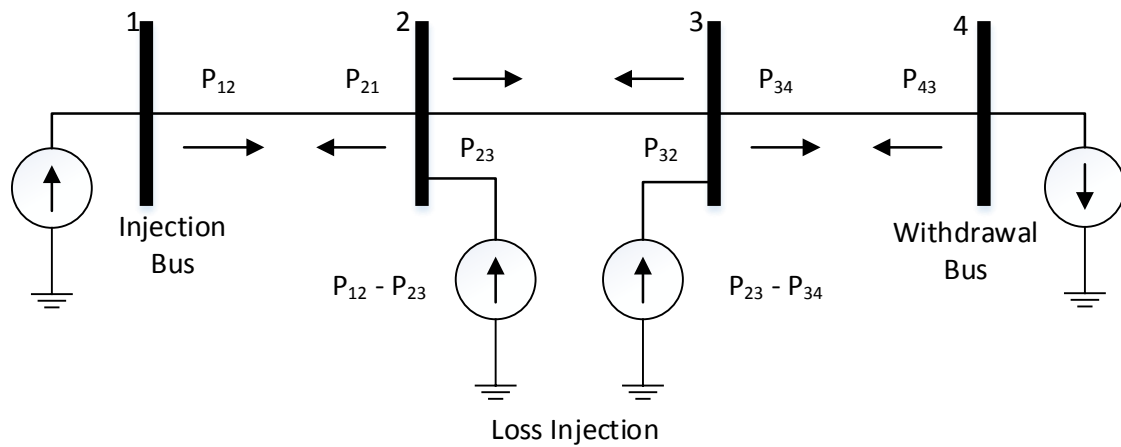
Figure 3.3 Loss modeled as Injections (Positive/Negative)

Inherently ac PTDFs are inconsistent and each column of ac PTDF's, i.e., injection

shift factor, can be made self-consistent (but not mutually consistent) if the branch

power loss is modeled as a power injection/withdrawal at one end of each branch, as

shown in Figure 3.3. This compensation of losses modeled as injection/withdrawal

accounts for the inconsistency due to resistive elements in the network. Define the in-

jection at bus k needed to compensate for branch losses associated with the qth injection

shift factor as ΔP_k^q :

$$\Delta P_k^q = - \ (\sum P_{k\_sending}^q - \sum P_{k\_receiving}^q) \tag{3.31}$$

where,

$\sum P^q_{k\_sending}$ = Sum of power received at node k from all branches where k is the

sending end node based on direction of the power flow

$\sum P^q_{k\_receiving}$ = Sum of power received at node k from all branches where k is the

receiving end node direction of the based on power flow

Define injection vector $\psi^{'q}$ associated with the qth injection shift factor can be

written as:

$$\psi^{'q} = \left[\Delta P^q_1, \Delta P^q_2, \ldots, \Delta P^q_k, \ldots \Delta P^q_N\right]^T \tag{3.32}$$

Combining all the injection vectors corresponding to each injection shift factor into

a matrix

$$\psi = \begin{bmatrix} \Delta P^1_1 & \cdots & \Delta P^i_1 & \cdots & \Delta P^N_1 \\ \vdots & \ddots & \vdots & \ddots & \vdots \\ \Delta P^1_j & \cdots & \Delta P^i_j & \cdots & \Delta P^N_j \\ \vdots & \ddots & \vdots & \ddots & \vdots \\ \Delta P^1_N & \cdots & \Delta P^i_N & \cdots & \Delta P^N_N \end{bmatrix}_{N \times N} \tag{3.33}$$

Using this matrix, the relationship between ac PTDF, derived dc PTDF and injection

matrix can be written as:

$$
\begin{bmatrix} \phi_m^{ac^1} \\ \phi_m^{ac^2} \\ \vdots \\ \phi_m^{ac^i} \\ \vdots \\ \phi_m^{ac^N} \end{bmatrix}_{(N \times 1)} = [\psi]_{N \, X \, N}^T \cdot \begin{bmatrix} \phi_m^{dc^1} \\ \phi_m^{dc^2} \\ \vdots \\ \phi_m^{dc^i} \\ \vdots \\ \phi_m^{dc^N} \end{bmatrix}_{(N \times 1)}
\tag{3.34}
$$

Solving this equation for the dc injection shift factors yields,

$$
\begin{bmatrix} \phi_m^{dc^1} \\ \phi_m^{dc^2} \\ \vdots \\ \phi_m^{dc^i} \\ \vdots \\ \phi_m^{dc^N} \end{bmatrix}_{(N \times 1)} = \left[[\psi]_{N \, X \, N}^T \right]^{-1} \cdot \begin{bmatrix} \phi_m^{ac^1} \\ \phi_m^{ac^2} \\ \vdots \\ \phi_m^{ac^i} \\ \vdots \\ \phi_m^{ac^N} \end{bmatrix}_{(N \times 1)}
\tag{3.35}
$$

where,

ϕ^{dc} = derived dc PTDF matrix

ϕ^{ac} = inconsistent ac PTDF matrix

m = represents m^{th} branch

ψ^T = transpose of the loss injection matrix

$\phi_m^{ac^i}$ = represents the ac PTDF corresponding to m^{th} branch for i^{th} ISF

$\phi_m^{dc^i}$ = represents the dc PTDF corresponding to m^{th} branch for i^{th} ISF

$$[\phi^{ac}]_{(L \times N)} = \begin{bmatrix} \phi_1^{ac^1} & \phi_1^{ac^2} & \cdots & \phi_1^{ac^N} \\ \phi_2^{ac^1} & \phi_2^{ac^2} & \cdots & \phi_2^{ac^N} \\ \vdots & \vdots & \cdots & \vdots \\ \phi_m^{ac^1} & \phi_m^{ac^2} & \cdots & \phi_m^{ac^N} \\ \vdots & \vdots & \vdots & \vdots \\ \phi_L^{ac^1} & \phi_L^{ac^2} & \cdots & \phi_L^{ac^N} \end{bmatrix}_{(L \times N)} \qquad (3.36)$$

$$[\phi^{dc}]_{(L \times N)} = \begin{bmatrix} \phi_1^{dc^1} & \phi_1^{dc^2} & \cdots & \phi_1^{dc^N} \\ \phi_2^{dc^1} & \phi_2^{dc^2} & \cdots & \phi_2^{dc^N} \\ \vdots & \vdots & \cdots & \vdots \\ \phi_m^{dc^1} & \phi_m^{dc^2} & \cdots & \phi_m^{dc^N} \\ \vdots & \vdots & \vdots & \vdots \\ \phi_L^{dc^1} & \phi_L^{dc^2} & \cdots & \phi_L^{dc^N} \end{bmatrix}_{(L \times N)} \qquad (3.37)$$

Equation (3.35) can be used to calculate the PTDFs corresponding to every injection bus corresponding to each branch one at a time. Linear system of equations (3.35) is solved using LU factorization and forward/backward substitution to calculate the dc PTDFs. Using the process each injection shift factor comprising the dc PTDFs are self-consistent but are not mutually consistent.

3.6   OBTAINING THE DC NETWORK MODEL

Now, the next problem that needs to be attacked is finding the equivalent line reactances for each branch using the above derived equivalent dc PTDF matrix. As stated above, the injection shift factors (ISF) derived corresponding to these derived dc PTDFs are inconsistent among themselves i.e. no single network reactances can satisfy all the ISFs simultaneously.

The problem then is to calculate the network reactances that can fit all of these derived dc PTDFs simultaneously as closely as possible. Using the derived dc PTDFs (ϕ^{dc}) to compute the Λ matrix in place of classical dc PTDFs (ϕ) in (3.29), is given by:

$$\min_{x} \left\| \Lambda \cdot [1/x] \right\|_2 \tag{3.38}$$

$$s.t. \qquad \left\| \frac{1}{x} \right\|_2 \geq Z \qquad Z > 0 \tag{3.39}$$

where, Z is an arbitrary small constant representing a lower bound on the L2 norm of vector (1/x) and Λ is the matrix defined by (3.33).

In addition to (3.38) , constructing an optimization approach which avoids the trivial solution to this optimization problem can be handled in several ways, such as an eigenvalue approach as discussed in [15]. Since all the susceptances can be scaled proportionally, a constraint (as per (3.39)) has been introduced for the purposes.

Let us define the vector of network susceptances as,

$$y = [y_1, y_2 \ldots y_i \ldots, y_L]^T \qquad y_i = 1/x_i \tag{3.40}$$

The constraint in (3.39) can be re-written with susceptance as:

$$y^T \cdot y \geq Z \tag{3.41}$$

Alternatively we define (3.45) as:

$$f(y) = y_1^2 + y_2^2 + \cdots + y_L^2 - Z \qquad \forall Z > 0 \tag{3.42}$$

In order to solve the problem in a linear least-squares sense, the constraint in (3.41) or (3.46) is linearized by using the first two terms of a Taylor-series expansion around the base-point, i.e. higher order terms are neglected. The base point for the susceptance is selected as:

$$y^{(o)} = [y_1^{(o)}, y_2^{(o)} \ldots y_i^{(o)} \ldots, y_L^{(o)}]^T \tag{3.43}$$

The truncated Taylor-series expansion of constraint is written as:

$$2 \cdot [y_1^{(o)}(y_1 - y_1^{(o)}) + y_2^{(o)}(y_{21} - y_2^{(o)}) + \cdots \\ + y_L^{(o)}(y_L - y_L^{(o)})] + y_1^{(o)2} + y_2^{(o)2} + \cdots + y_L^{(o)2} - Z = 0 \tag{3.44}$$

Upon further simplification, this yields

$$2 \cdot [y_1^{(o)} \cdot y_1 + y_2^{(o)} \cdot y_2 + \cdots + y_L^{(o)} \cdot y_L] = \\ y_1^{(o)2} + y_2^{(o)2} + \cdots\cdots + y_L^{(o)2} + Z \tag{3.45}$$

This linearized constraint can be embedded into (3.38) as,

$$\begin{bmatrix} 2y_1^{(j-1)} & 2y_2^{(j-1)} & \cdots & 2y_L^{(j-1)} \\ \cdots & \cdots & \cdots & \cdots & \cdots \\ & & \Lambda & \\ \cdots & \cdots & \cdots & \cdots & \cdots \end{bmatrix}_{N \cdot L + 1 \times L} \cdot [y^{(j)}] = \begin{bmatrix} \sum_i y_i^{(j-1)2} + Z \\ 0 \\ \vdots \\ 0 \end{bmatrix} \tag{3.46}$$

where,

(j) = 1, 2…, m iteration index

This equation can be restated as:

$$\Lambda' \cdot [y] = b \tag{3.47}$$

41

which is a set of over-determined linear equations; therefore the solutions is an error

minimization process.

$$[y]^{(j)} = [(\Lambda'^{(j-1)T} \cdot \Lambda'^{(j-1)})]^{-1} \cdot [\Lambda'^{(j-1)}]^T b^{(j-1)} \qquad (3.48)$$

Also, note that $(\Lambda'^{(j-1)T} \cdot \Lambda'^{(j-1)})$ is a square matrix of cardinality $L \times L$ and it is a very

sparse matrix, so one can exploit the benefits of the sparsity techniques to evaluate

(3.48). This calculation using sparse LU factorization and forward/backward

substitution is computationally more efficient than the eigenvalue decomposition, QR

factorization method proposed in [15]. Equation (3.47) is solved recursively to obtain

better estimates of the network parameters (y) at each iteration. Equation (3.47) is

iterated until the convergence tolerance ε (10^{-4}) is met.

$$\max(abs.|y^{(j)} - y^{(j-1)}|) < \varepsilon \qquad (3.49)$$

It is worthwhile to note that the rank of the lambda (Λ) matrix may vary with the

network topology and this subject shall be elaborated upon more in the next chapter.

3.7   SUMMARY

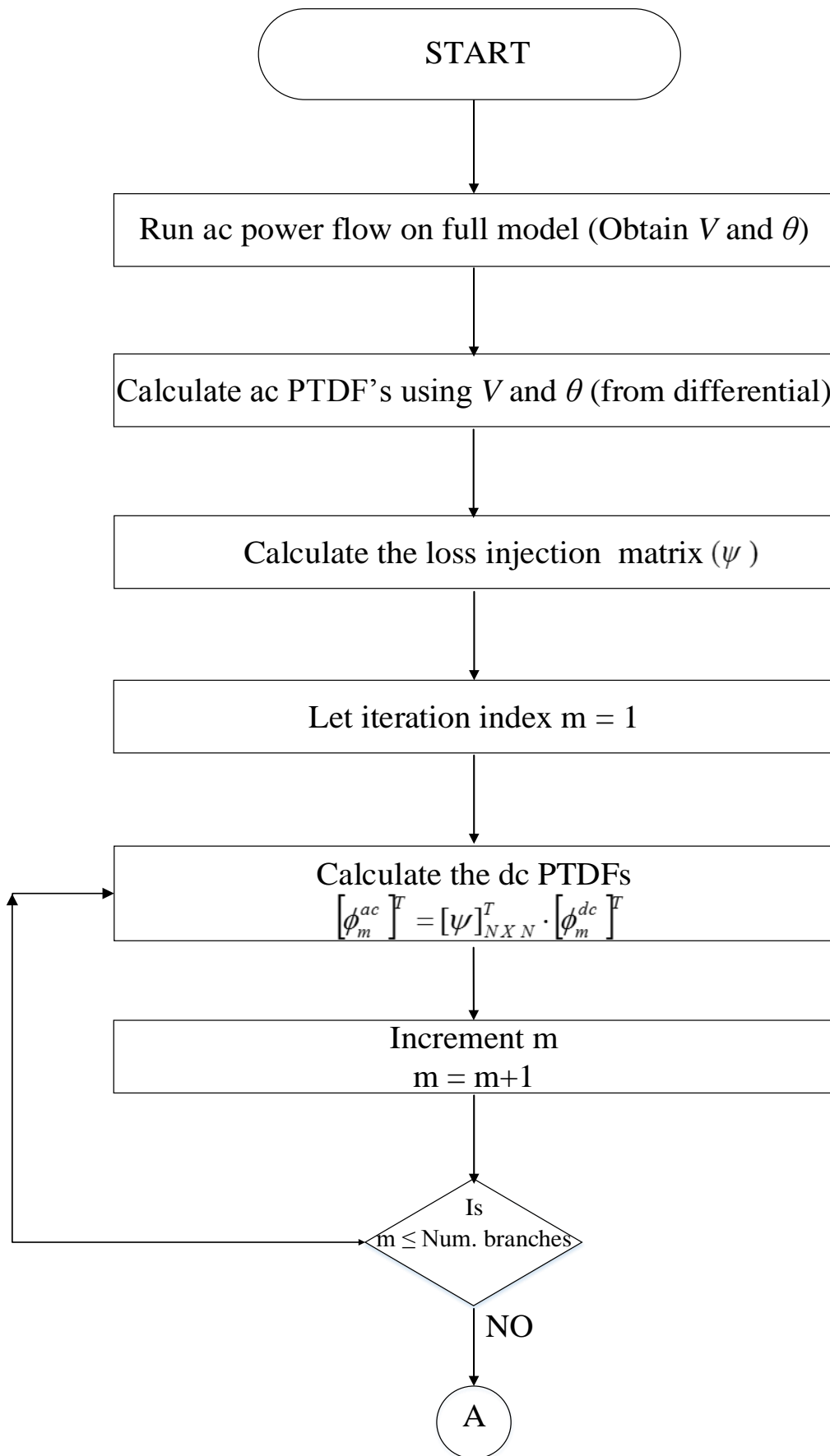In this chapter, a PTDF based dc network model development procedure is

introduced. The proposed model is a least square based evaluation technique for

deriving network parameters. It is worth mentioning, that several tests were conducted

for optimal performance at both the stages i.e. equivalent dc PTDF calculation and

evaluation of network parameters in the derivation of the proposed model. In the

derivation of dc PTDFs several possibilities of including weighted power flow constraints in (3.34) was explored. While several optimization techniques such as L1 norm, least absolute value approach and L-infinity were introduced for (3.38)-(3.39) to derive equivalent model parameters. These variations in optimization techniques were evaluated for power flows at the base operating condition and under contingency analysis. Also, the eigenvalue approach described in [15] was implemented and tested for (3.38)-(3.39). It was found that network parameters obtained using the least square approach and eigenvalue approach yielded same results (although scaled) within the precision of $1e^{-3}$. It can be concluded the least square approach and eigenvalue approach performed better than the other optimization techniques mentioned above when evaluated for distribution of power flows in network under contingency conditions. Furthermore, it is essential to note that eigenvalue approach is computationally much more expensive (as it involves singular value decomposition) than performing least squares.

The model development process can be summarized in the flowchart shown in Figure 3.4.
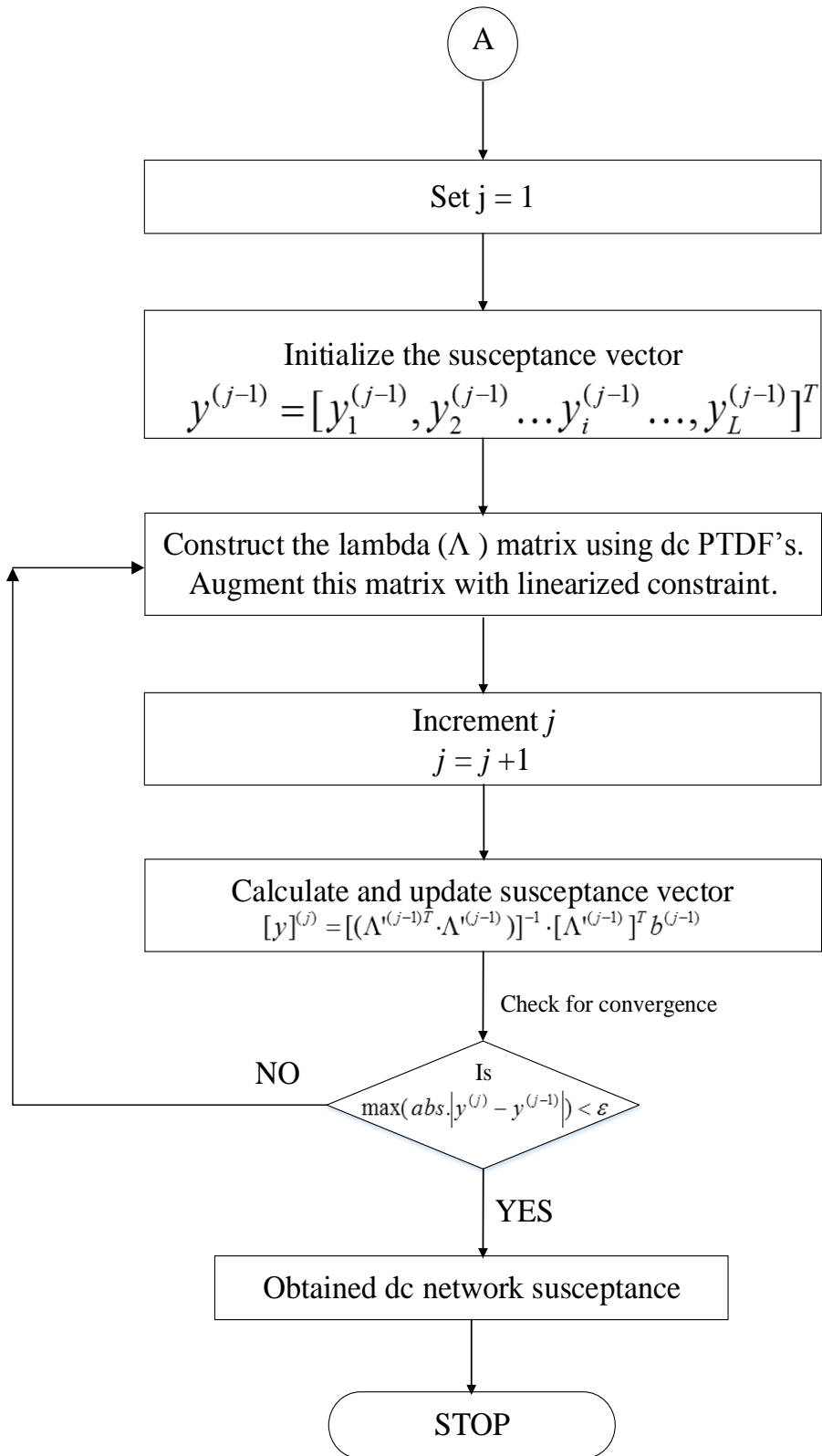
```
                      ┌─────────────────────┐
                      │        START        │
                      └─────────────────────┘
                                 │
                                 ▼
        ┌───────────────────────────────────────────────────┐
        │   Run ac power flow on full model (Obtain V and θ) │
        └───────────────────────────────────────────────────┘
                                 │
                                 ▼
        ┌───────────────────────────────────────────────────┐
        │ Calculate ac PTDF's using V and θ (from differential)│
        └───────────────────────────────────────────────────┘
                                 │
                                 ▼
        ┌───────────────────────────────────────────────────┐
        │   Calculate the loss injection  matrix (ψ )        │
        └───────────────────────────────────────────────────┘
                                 │
                                 ▼
        ┌───────────────────────────────────────────────────┐
        │   Let iteration index m = 1                        │
        └───────────────────────────────────────────────────┘
                                 │
                                 ▼
        ┌───────────────────────────────────────────────────┐
        │            Calculate the dc PTDFs                  │
        │                                                   │
        └───────────────────────────────────────────────────┘
```

Calculate the dc PTDFs

$$\left[\phi_m^{ac}\right]^T = [\psi]_{N\,X\,N}^T \cdot \left[\phi_m^{dc}\right]^T$$

Increment m

$$m = m+1$$

Is
$$m \leq \text{Num. branches}$$

NO

A

A

Set j = 1

Initialize the susceptance vector

$$y^{(j-1)} = [y_1^{(j-1)}, y_2^{(j-1)} \ldots y_i^{(j-1)} \ldots, y_L^{(j-1)}]^T$$

Construct the lambda (Λ) matrix using dc PTDF's. Augment this matrix with linearized constraint.

Increment j
$$j = j + 1$$

Calculate and update susceptance vector
$$[y]^{(j)} = [(\Lambda^{'(j-1)T} \cdot \Lambda^{'(j-1)})]^{-1} \cdot [\Lambda^{'(j-1)}]^T b^{(j-1)}$$

Check for convergence

NO

Is
$$\max(abs.|y^{(j)} - y^{(j-1)}|) < \varepsilon$$

YES

Obtained dc network susceptance

STOP

Figure 3.4 Flowchart for entire network equivalencing process

4   MODEL VALIDATION AND NUMERICAL ILL-CONDITIONING

4.1   INTRODUCTION

In the previous chapter, a novel network equivalence technique has been proposed. This model provides the network equivalent when the lambda (Λ) matrix (prior to augmenting it with constraint) is rank deficient by only one degree. However, depending on the topology, the rank deficiency of Λ-matrix may be greater than one. This leads to a theoretically undetermined problem, though due to imprecision in the PTDF's the matrix will appear to be of full rank, but numerically ill-conditioned, leading to erroneous results for the value of the network susceptances.

The focus of this chapter is on validating the proposed model and analyzing the topological dependency of rank of the lambda (Λ) matrix and on how to resolve the rank deficiency issues. The approach to identify topological rank dependency is studied empirically.

4.2   MODEL VALIDATION

Model validation of the physical network which includes resistance, phase-shifting transformers using the proposed method is a daunting task. This is attributed to the use of ac PTDFs which include the inherent nonlinearities, such as losses, typical of such network. Thus the network parameters derived from the proposed model cannot be compared against any reference. Therefore, some sanity-check exercises are introduced for algorithmic verification purposes on a small

46

system, before the application of this technique on the larger and realistic power systems. Since the proposed model is derived in two stages i.e. first, obtaining the equivalent dc PTDFs from ac PTDFs and, second, deriving network susceptances using these derived dc PTDFs, the sanity check of this proposed model is also segregated into two independent parts.

4.2.1 CHECKS ON THE EQUIVALENT DC PTDFs

The classical dc PTDFs, which are completely consistent, are different than the derived dc PTDFs, which are consistent within a shift factor but inconsistent across shift factors. As an example, consider a non-branching radial network. In this network, the power distribution is unidirectional i.e. power will flow from the source or the injection bus to the sink bus. Therefore, the derived dc PTDFs and ac PTDFs should converge to a same value. This simple validation experiment exploits the topological property of the radial network.
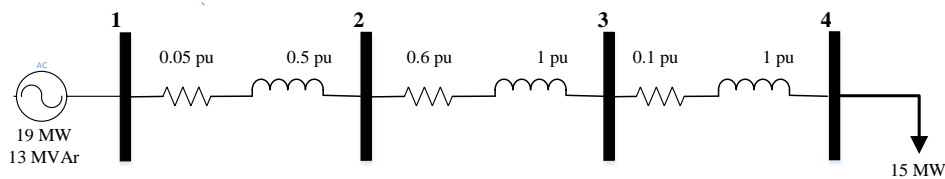
Figure 4.1 Radial network of four buses

For the sample radial network show in Figure 4.1, an ac power flow is run to compute the bus voltage magnitudes and angles. Based on the network parameters and ac solution, the ac PTDFs are computed as discussed in previous chapter. Bus 4 is

47

the slack bus or the sink bus. The ac PTDFs at the *from* end for the shown network is

given by:

$$ac\ PTDF_{from} = \begin{bmatrix} Line & | Inj.\,Bus & 1 & 2 & 3 \\ L-12 & & 1.5349 & 0 & 0 \\ L-23 & & 1.4504 & 0.9669 & -0.0237 \\ L-34 & & 0.4365 & 0.3114 & 0.6925 \end{bmatrix}$$

It is worth noting that the ac PTDFs can achieve PTDF values greater than 1 due to the

sensitivities of the ac model or insertion of series capacitors (often used in the line

compensation). Using the proposed model, the dc PTDFs are obtained as:

$$dc\ PTDF = \begin{bmatrix} Line & | Inj.\,Bus & 1 & 2 & 3 \\ L-12 & & 1 & 0 & 0 \\ L-23 & & 1 & 1 & 0 \\ L-34 & & 1 & 1 & 1 \end{bmatrix}$$

This is what we expect the model to deliver, for the radial network i.e. the power from

the injected bus flows to the sink bus. Note that the dc PTDFs have a maximum value

equal to 1.0. The dc PTDFs can also attain values greater than 1.0 in cases where

negative susceptances are introduced in the model i.e. insertion of series capacitors for

line compensation.

4.2.2   TOWARD   VALIDATING   THE   SUSCEPTANCE   EVALUATION
         ALGORITHM

Since the dc PTDFs obtained using the proposed algorithm are inconsistent across

the shift factors, the validation of the reactance/susceptance computation algorithm

becomes a thorny issue: how does one compare the obtained dc reactances with the

given network ac parameters? Thus, for the purpose of algorithm validation the classical dc PTDFs are used to compute the lambda (Λ) matrix instead of the derived dc PTDFs as explained in the proposed model.

As stated earlier, the classical dc PTDFs are fully consistent along and across the shift factors. This will result in a unique solution reactance vector. As stated earlier, the angle of this reactance vector is unique, though it can be scaled in magnitude without altering its "current division" properties. One way of partially validating the approach is to use (3.29) while replacing ϕ by the classical dc PTDFs of the network. Then, using the initial estimate as per (3.43) and solving for susceptances using (3.46) – (3.48), the solution will be the susceptances of the original network. Consider a small 3-bus example for illustration.
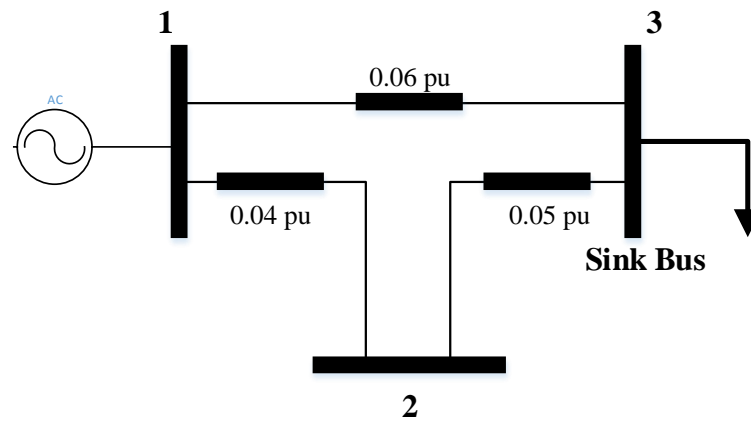
Figure 4.2 Three bus sample system

The classical dc PTDFs are given by (3.9):

$$
Classical\ dc\ PTDF =
\begin{bmatrix}
Line & Inj.\,Bus & 1 & 2 \\
L-12 & & 0.4 & -0.3333 \\
L-13 & & 0.6 & -0.3333 \\
L-32 & & -0.4 & -0.6667
\end{bmatrix}
$$

The corresponding lambda (Λ) matrix derived using (3.29) is

$$\Lambda = \begin{bmatrix} -0.2667 & 0.4 & 0 \\ 0.2667 & -0.4 & 0 \\ 0.2667 & -0.4 & 0 \\ 0.2667 & 0 & -0.3333 \\ -0.2667 & 0 & 0.3333 \\ -0.2667 & 0 & 0.3333 \end{bmatrix}$$

Using the initial estimate of susceptances $y = [1, 1, 1]^T$; and augmenting the lambda

(Λ) matrix with the linearized constraint, the linear system of equations is solved as

per (3.46)-(3.48). The converged solution is given by:

$y = [1.1997, 0.7998, 0.9597]^T$

The value of the susceptance vector based on classical dc model reactances is given

by:

$y = [25, 16.6667, 20]^T$

It can be noticed that the susceptance values are scaled by a factor of 20.84.

Therefore, if the solution is scaled up by a common multiplying factor for all the

susceptances then the original susceptances are obtained. In this case a random initial

value was chosen which illustrates that the robustness of this algorithm and

non-dependency of solution on initial point. However, for fast convergence a more

appropriate initial point such as susceptance vector corresponding to the classical dc

reactance could be chosen.

The same test was conducted on IEEE-118 bus system and ERCOT for validation

purposes and similar test results were obtained.

4.3 PROBLEMS ASSOSCIATED WITH RANK DEFICIENCY

In the proposed modeling process, the reactances are evaluated by solving the over-determined set of linear equations whose coefficients are described by the Λ -matrix and b vector. If the Λ - matrix becomes theoretically singular then the condition number goes to infinity. In practical problems, due to roundoff error, theoretically singular matrices will appear nonsingular but will have very large condition numbers, which allows the calculations to go forward but results in an erroneous answer. In the next sections the cause of such rank deficiency in the Λ -matrix is explored.

4.4 TOPOLOGICAL DEPENDENCY OF THE RANK OF Λ

Let us first revisit the mathematical concept of the rank of the matrix. For the matrix A of cardinality m by n

Row rank: Is the maximum number of linearly independent rows in the matrix.

Row rank of $A \leq m$

Column rank: Is the maximum number of linearly independent columns in the matrix.

Column rank of $A \leq n$

rank $(A) \leq$ min*(m,n)*

Also, by linear algebra

rank $(A) =$ rank (A^T)

Suppose two matrices A and B have rank as m and n respectively. Then

rank $(A.B) =$ min(rank(A), rank(B))

This property shall be exploited as the Λ - matrix size grows with the increase in the system size (recall that the cardinality of Λ = $N.L \times L$). The problem at hand involves the solution to the over-determined set of equations, whose solution is given by (3.48) re-written here as:

$$[y]^{(j)} = [(\Lambda'^{(j-1)T} \cdot \Lambda'^{(j-1)})]^{-1} \cdot [\Lambda'^{(j-1)}]^T b^{(j-1)}$$

Finding the rank of Λ is much more computationally expensive than that of $\Lambda^T \cdot \Lambda$ which has cardinality of $L \times L$. Therefore, $\Lambda^T \cdot \Lambda$ is used to compute rank of Λ.

4.4.1   EMPIRICAL ANALYSIS OF NETWORK TOPOLOGIES

Consider the following network topologies for which the rank of the Λ matrix is determined and tabulated. This empirical approach will lead to an intuitive understanding of the relationship between the rank of Λ and the network topology.

Case 1: Radial network
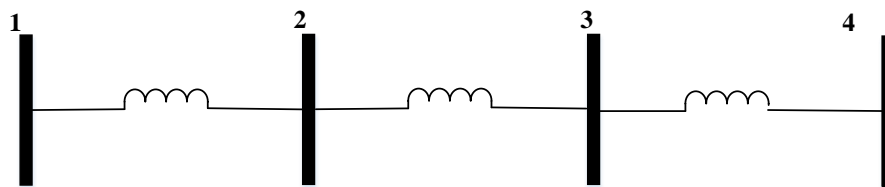
Figure 4.3 Four bus sample radial network

rank (Λ) = 0

An important conclusion can be drawn from this result is that it is impossible to determine the network parameters for a radial network. Also, it aligns with our intuitive understanding of the radial network that the power flow is independent of the

52

network reactance. Therefore, network branch parameters need to be specified for such a network.

Case 2: Meshed network

Let us now merge bus 1 and bus 4 from the previous network.
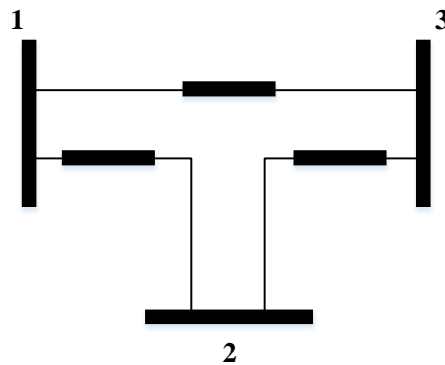
Figure 4.4 Three bus meshed network

rank (Λ) = 2 (The rank of Λ-matrix for network shown in Figure 4.4 is two.)

Thus, in a meshed network if the linearized constraint ((3.45)-(3.46)) is included then the equivalent network branch parameters can be calculated using the proposed algorithm.

Case 3: Semi-meshed network

For the 8-bus model shown in Figure 4.5 the naively expected rank of the Λ matrix is 8 (Number of branches - 1). However, the actual rank turns out to be 5. This aligns with our intuition that radial lines (2 in number) and radially-attached sub-networks (buses 5, 6, 7 and 8) reduce the rank of the matrix by 1 degree each.
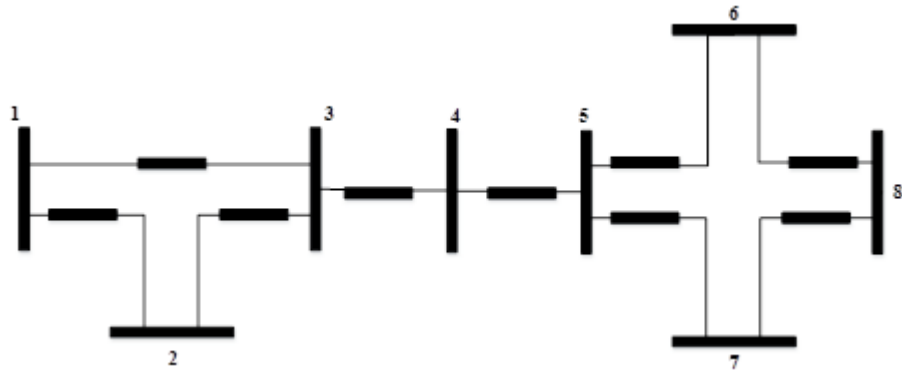
Figure 4.5 Eight bus meshed network

We observe that it is not necessary that the sub-networks be connected only through radial lines but can be connected radially on the bus itself as shown in Figure 4.6.
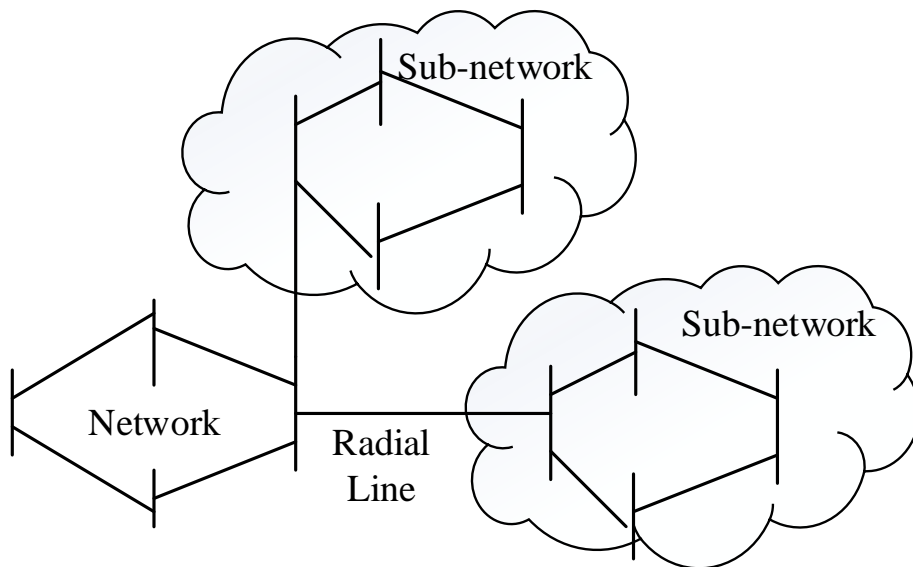
Figure 4.6 Generalized network

4.5   IDENTIFICATION OF THE SUB-NETWORKS

Now that some sense for the cause of numerical ill-conditioning or rank deficiency due to network topology of the Λ matrix is developed, it becomes

convenient to use a larger network to identify the radial lines and sub-networks using an algorithm.
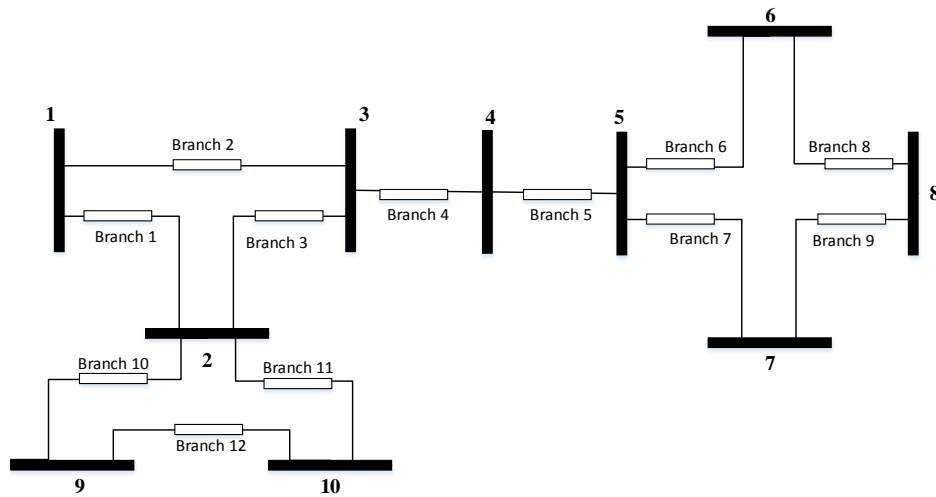
Figure 4.7 10-bus network

Consider the 10-bus sample network shown in Figure 4.7 with bus 10 serving as the sink bus. Assume that the network is lossless and all the reactances are set to 1 per unit. The classical dc PTDF matrix is computed for the network shown in Figure 4.7 using (3.9) as shown in Table 4.1.

This dc PTDF matrix structure can help decipher our empirical observations from the previous section. The following key characteristics are observed in the dc PTDF matrix:

- Strictly radial branches have PTDF values of either 0 or 1 (branch 4 and 5);
- Identify the pattern of non-zero PTDFs in non-radial branches i.e. rows in the PTDF matrix other than the rows of the PTDF matrix representing radial branch. (i.e. in essence make note of for which injection buses there is flow over the branch). Branches corresponding to PTDF matrix which have same pattern of non-zero PTDF shall form a sub-network.

For example:

55

Branches/Line – 1, 2 and 3 have the same pattern of non-zero elements.

Branches/Line – 6, 7, 8 and 9 have the same pattern of non-zero elements.

Branches/Line – 10, 11 and 12 have the same pattern of non-zero elements.

From this observation, it can be concluded that branches (1, 2 and 3) form one sub-network, branches (6, 7, 8 and 9) form the second sub-network and branches (10, 11 and 12) form the third sub-network in the network. Also branches 4 and 5 are the radial branches in the network.

For the network shown in Figure 4.7 the rank (Λ) = 7. For a 12-branch network, the Λ-matrix is deficient by a degree of 5, which exactly matches our conclusion (3 sub-networks + 2 radial branches.)

Table 4.1 Classical dc PTDFs for network in figure 4.7

Line	From	To	1	2	3	4	5	6	7	8	9
1	1	2	0.6667	0	-0.3333	0.3333	0.3333	0.3333	0.3333	0.3333	0
2	1	3	0.3333	0	-0.3333	-0.3333	-0.3333	-0.3333	-0.3333	-0.3333	0
3	2	3	-0.3333	0	-0.6667	-0.6667	-0.6667	-0.6667	-0.6667	-0.6667	0
4	3	4	0	0	0	-1	-1	-1	-1	-1	0
5	4	5	0	0	0	0	-1	-1	-1	-1	0
6	5	6	0	0	0	0	0	-0.75	-0.25	-0.5	0
7	5	7	0	0	0	0	0	-0.25	-0.75	-0.5	0
8	6	8	0	0	0	0	0	0.25	-0.25	-0.5	0
9	7	8	0	0	0	0	0	0.25	0.25	-0.5	0
10	2	9	0.3333	0.3333	0.3333	0.3333	0.3333	0.3333	0.3333	0.3333	-0.3333
11	2	10	0.6667	0.6667	0.6667	0.6667	0.6667	0.6667	0.6667	0.6667	0.3333
12	9	10	0.3333	0.3333	0.3333	0.3333	0.3333	0.3333	0.3333	0.3333	0.6667

4.6 EQUIVALENT NETWORK SOLUTION WITH SUB-NETWORKS

Upon identification of radial lines and sub-networks the problem at hand is to evaluate the equivalent dc PTDFs using the rank deficient Λ matrix. The network parameter evaluation process can be divided into sub-problems, each of whose Λ matrices are rank deficient by one:

- Fix the susceptance of the radial lines arbitrarily.
- Solve each independent sub-network one at a time.

For example, in the network shown in Figure 4.7 the subsequent steps are followed:

1) Set the radial branches 4 and 5 to classical dc reactance.
2) Then calculate the Λ-matrix using the subset of the PTDF matrix associated with each of the sub-networks (Sub Network – 1: 1, 2 and 3; Sub Network – 2: 2, 9 and 10; Sub Network – 3: 5, 6, 7 and 8).

$$\Lambda_S \cdot \left[\frac{1}{x_S} \right] = 0 \tag{4.1}$$

where,

$$\Lambda_S = \begin{bmatrix} (\phi_S \cdot C_S^T - I) \cdot diag(c_{1_S}) \\ (\phi_S \cdot C_S^T - I) \cdot diag(c_{2_S}) \\ \dots\dots\dots\dots\dots \\ (\phi_S \cdot C_S^T - I) \cdot diag(c_{N_S}) \end{bmatrix}$$

S = Subscript S indicates the values corresponding to the sub-networks.

3) The Λ_S matrix thus formed is augmented with the constraint as explained in section 3.6. An initial estimate of susceptances is chosen for branches in each sub-network. The susceptance of a network model corresponding to each of the

sub-network is calculated using the iterative procedure described in previous

chapter.

4.7   SUMMARY

In this chapter, model validation of the proposed model was explored and then the

problems associated with the rank deficiency of Λ-matrix were discussed. The following

flowchart (Figure 4.8) schematically summarizes the procedure to identify the

sub-networks and evaluation of the network parameters. It is found that even for very

large networks such sub-networks are not very large in number and size. Therefore, it is

not very computationally expensive to evaluate such sub-networks.
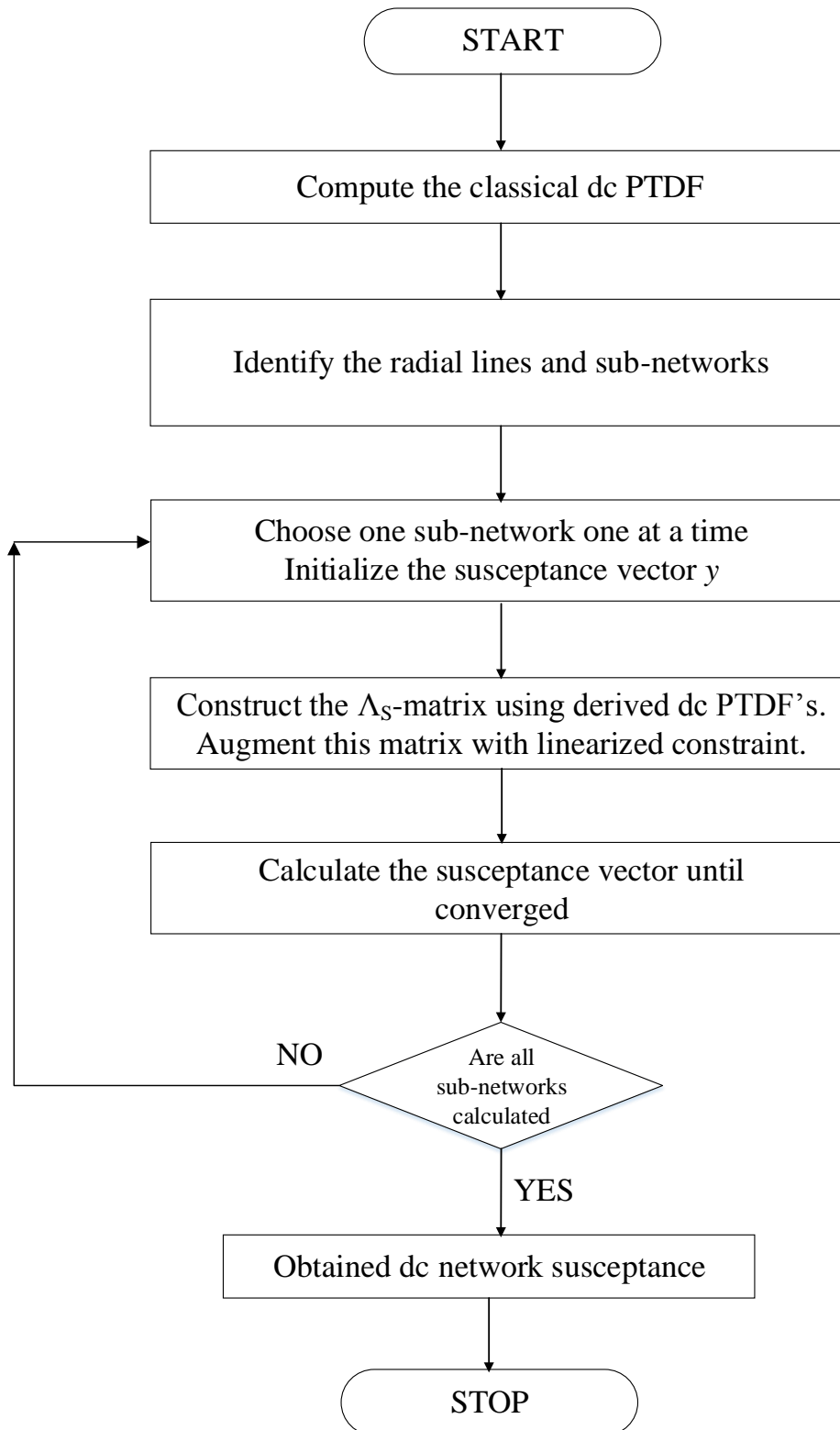
Figure 4.8 Flowchart for sub-network reactance evaluation

5 NUMERICAL EXAMPLES

5.1 INTRODUCTION

This chapter presents the implementation of the concepts developed through numerical examples. Since the accuracy and performance of dc models are subject to the assumptions made during the modeling stage and loading levels (i.e. lightly loaded or heavily loaded) of the system. Therefore, an attempt has been made to develop general insight for these dc models. The accuracy of several parameters like branch power flows during contingency conditions, PTDF's, branch reactance were evaluated for a 7-bus, the IEEE-118 and the 5650 bus ERCOT interconnection to draw comparison between different models currently in use (i.e. classical dc, single multiplier and proposed model) described earlier.

5.2 CASE STUDIES AND DESCRIPTION

This section summarizes the general information of the three cases illustrated:

Table 5.1 Case Study details

S. No.	Case Description	Buses	Branches	Radial Branches
1	7-Bus	7	11	0
2	IEEE-118	118	186	9
3	ERCOT	5650	6771	1892

5.2.1 Case Study 1: 7-Bus Model

Figure 5.1 shows the 7-bus, 11-branch network model. The network parameters are given in Table 5.2 for reference.
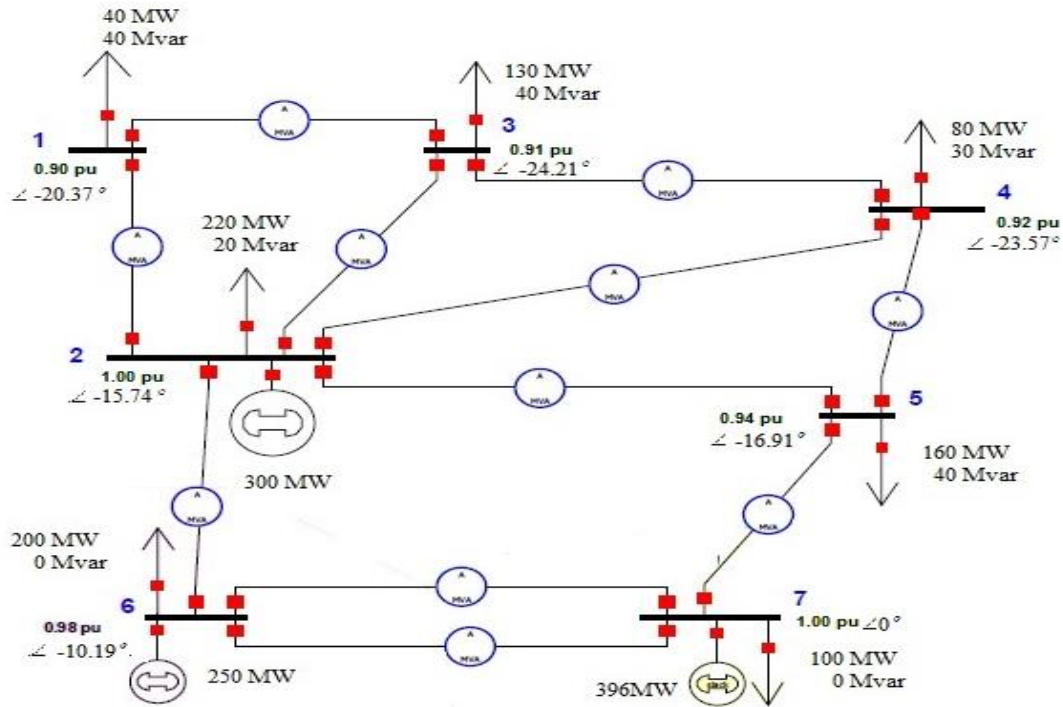
Figure 5.1 7-Bus Network Model

Table 5.2 Network Parameters for 7-bus model

Line No.	From Bus	To Bus	R (p.u.)	X (p.u.)	P[†] (MW)	Q[†] (MVAr)
1	1	3	0.02	0.24	22.25	-5.13
2	1	2	0.06	0.15	-62.25	-34.87
3	2	6	0.005	0.06	-153.52	53.79
4	2	5	0.01	0.12	20.11	48.63
5	2	4	0.015	0.18	73.1	45.86
6	2	3	0	0.18	74.27	56.85
7	3	4	0.015	0.03	-33.61	-5.59
8	4	5	0.02	0.24	-41.84	-3.55
9	6	7	0.25	0.25	-35.5	33.84
10	6	7	0	0.25	-69.35	-1.66
11	7	5	0.006	0.15	184.69	59.83

[†]measured at from bus

62

The ac PTDFs for the model are derived using (3.6) are shown in Table 5.3 and

Table 5.4.

Table 5.3 ac PTDFs (at sending end)

From Bus	To Bus	1	2	3	4	5	6
1	3	0.3492	0.0169	-0.1473	-0.1102	-0.0153	0.0125
1	2	0.6508	-0.0169	0.1473	0.1102	0.0153	-0.0125
2	6	0.5421	0.5215	0.5059	0.4915	0.3425	-0.3529
2	5	0.3315	0.3592	0.2458	0.2114	-0.2493	0.2649
2	4	-0.0637	0.0573	-0.2528	-0.3265	-0.0426	0.0422
2	3	-0.0998	0.0440	-0.3355	-0.2546	-0.0335	0.0324
3	4	0.2459	0.0607	0.5188	-0.3636	-0.0486	0.0448
4	5	0.1876	0.1176	0.2793	0.3144	-0.0905	0.0867
6	7	0.1602	0.1542	0.1496	0.1453	0.1012	0.1865
6	7	0.3907	0.3759	0.3646	0.3543	0.2469	0.4548
7	5	-0.5362	-0.4907	-0.5447	-0.5466	-0.6776	-0.3618

Table 5.4 ac PTDFs (at receiving end)

From Bus	To Bus	1	2	3	4	5	6
1	3	-0.3457	-0.0167	0.1457	0.1090	0.0151	-0.0123
1	2	-0.7101	0.0181	-0.1634	-0.1218	-0.0171	0.0133
2	6	-0.5510	-0.5300	-0.5142	-0.4995	-0.3481	0.3586
2	5	-0.3313	-0.3586	-0.2460	-0.2119	0.2471	-0.2645
2	4	0.0614	-0.0561	0.2459	0.3176	0.0413	-0.0414
2	3	0.0998	-0.0440	0.3355	0.2546	0.0335	-0.0324
3	4	-0.2490	-0.0614	-0.5252	0.3680	0.0492	-0.0453
4	5	-0.1914	-0.1198	-0.2849	-0.3208	0.0923	-0.0884
6	7	-0.2305	-0.2217	-0.2151	-0.2090	-0.1456	-0.2683
6	7	-0.3907	-0.3759	-0.3646	-0.3543	-0.2469	-0.4548
7	5	0.5227	0.4785	0.5309	0.5327	0.6605	0.3528

The equivalent dc PTDFs thus obtained using (3.35) are given in Table 5.5.

Table 5.5 Equivalent dc PTDFs

From Bus	To Bus	1	2	3	4	5	6
1	3	0.3484	0.0170	-0.1457	-0.1095	-0.0150	0.0127
1	2	0.6516	-0.0170	0.1457	0.1095	0.0150	-0.0127
2	6	0.5078	0.5207	0.4867	0.4786	0.3373	-0.3577
2	5	0.3116	0.3609	0.2394	0.2089	-0.2473	0.2694
2	4	-0.0659	0.0574	-0.2485	-0.3249	-0.0420	0.0428
2	3	-0.1020	0.0440	-0.3319	-0.2531	-0.0329	0.0329
3	4	0.2465	0.0610	0.5224	-0.3626	-0.0479	0.0455
4	5	0.1806	0.1184	0.2738	0.3125	-0.0899	0.0884
6	7	0.1477	0.1515	0.1416	0.1392	0.0981	0.1868
6	7	0.3601	0.3693	0.3452	0.3394	0.2392	0.4555
7	5	-0.4922	-0.4793	-0.5133	-0.5214	-0.6627	-0.3577

Also the classical dc PTDFs for the model are given for reference in Table 5.6.

Table 5.6 Classical dc PTDFs

From Bus	To Bus	1	2	3	4	5	6
1	3	0.3389	0.0202	-0.1512	-0.1160	-0.0164	0.0137
1	2	0.6611	-0.0202	0.1512	0.1160	0.0164	-0.0137
2	6	0.5457	0.5621	0.5194	0.5090	0.3550	-0.2959
2	5	0.2734	0.3192	0.2000	0.1710	-0.2588	0.2157
2	4	-0.0590	0.0546	-0.2407	-0.3126	-0.0442	0.0369
2	3	-0.0990	0.0439	-0.3276	-0.2514	-0.0356	0.0296
3	4	0.2399	0.0641	0.5212	-0.3674	-0.0520	0.0433
4	5	0.1809	0.1187	0.2805	0.3200	-0.0962	0.0802
6	7	0.2728	0.2811	0.2597	0.2545	0.1775	0.3521
6	7	0.2728	0.2811	0.2597	0.2545	0.1775	0.3521
7	5	-0.4543	-0.4379	-0.4806	-0.4910	-0.6450	-0.2959

Since the derived equivalent dc PTDFs and classical dc PTDFs correspond to the proposed model and more common prevalent models, respectively, their comparison is shown in Figure 5.2.
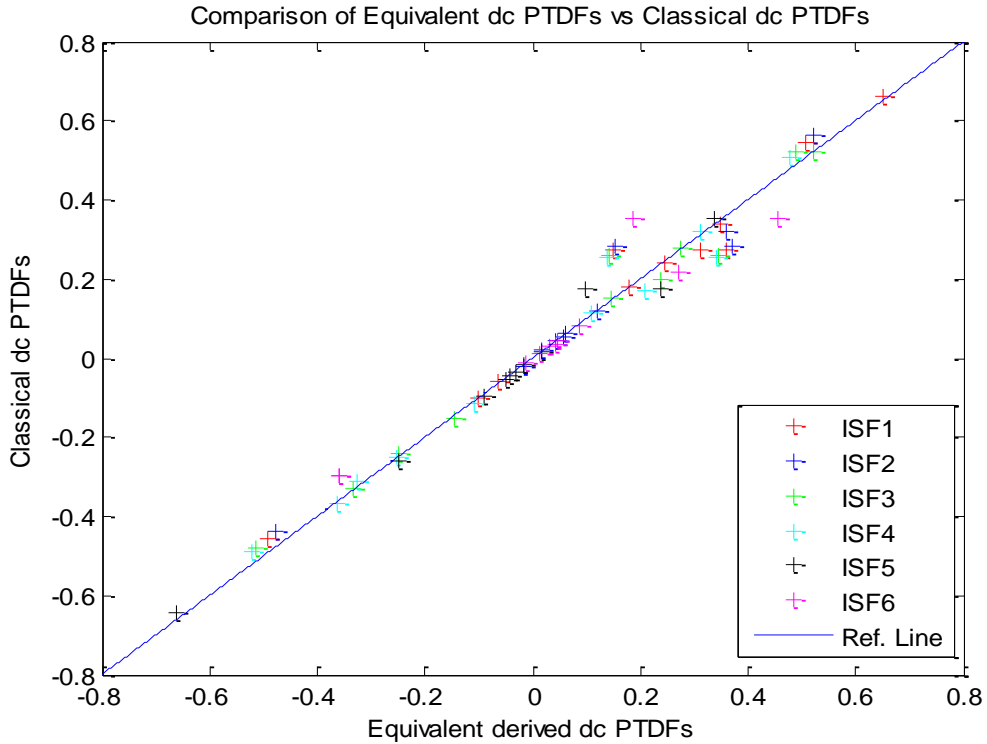
Figure 5.2 Comparison of Classical dc and Equivalent derived dc PTDFs

ISF1 – ISF6 in Figure 5.2 represent the injection shift factors (i.e. column vectors in PTDF matrix) corresponding to each non-sink bus for a 7-bus system. '+' represent each PTDF values along the injection shift factors. Figure 5.2 shows there is an offset in the two PTDFs values from the reference line (marked blue) which represent the slope of 45°. This is attributed to the variation of the reactance values thus obtained using the reactance evaluation algorithm described in Chapter 3 and Chapter 4.

The value of loss compensation in a single multiplier type dc model is computed using (2.13) and for this 7-bus system is given by:

Single Multiplier (γ) = 1.017

The reactances obtained using the proposed algorithm and the corresponding power flows at the base operating point are shown in Table 5.7 below:

Table 5.7 Reactance and power flow comparison at base operating point

From Bus	To Bus	X	X_{prop}	$PF_{Cl.\ dc}$	$PF_{SM.\ dc}$	PF_{prop}
1	3	0.24	0.24	20.31	20.49	22.25
1	2	0.15	0.1595	-60.31	-61.17	-62.25
2	6	0.06	0.0556	-156.71	-160.98	-153.52
2	5	0.12	0.1107	27.11	25.03	20.11
2	4	0.18	0.1675	71.95	72.73	73.1
2	3	0.18	0.1744	77.34	78.30	74.27
3	4	0.03	0.0302	-32.35	-33.41	-33.61
4	5	0.24	0.2429	-40.40	-42.04	-41.84
6	7	0.25	0.5628	-53.35	-57.19	-35.5
6	7	0.25	0.2308	-53.35	-57.19	-69.35
7	5	0.15	0.1504	173.29	179.73	184.69

$PF_{Cl.\ dc}$ = Classical dc; $PF_{SM.\ dc}$ = Single Multiplier; PF_{prop} = Proposed Model

The performance of various dc models under base-case operating conditions is compared against ac branch power flow solution. For this purposes, we define branch power flow error as:

$$Error = PF_{model} - PF_{ac} \tag{5.1}$$

Whereas,

PF_{model} = dc power flow for a given model (in MW)

PF_{ac} = ac power flow for the model (in MW)

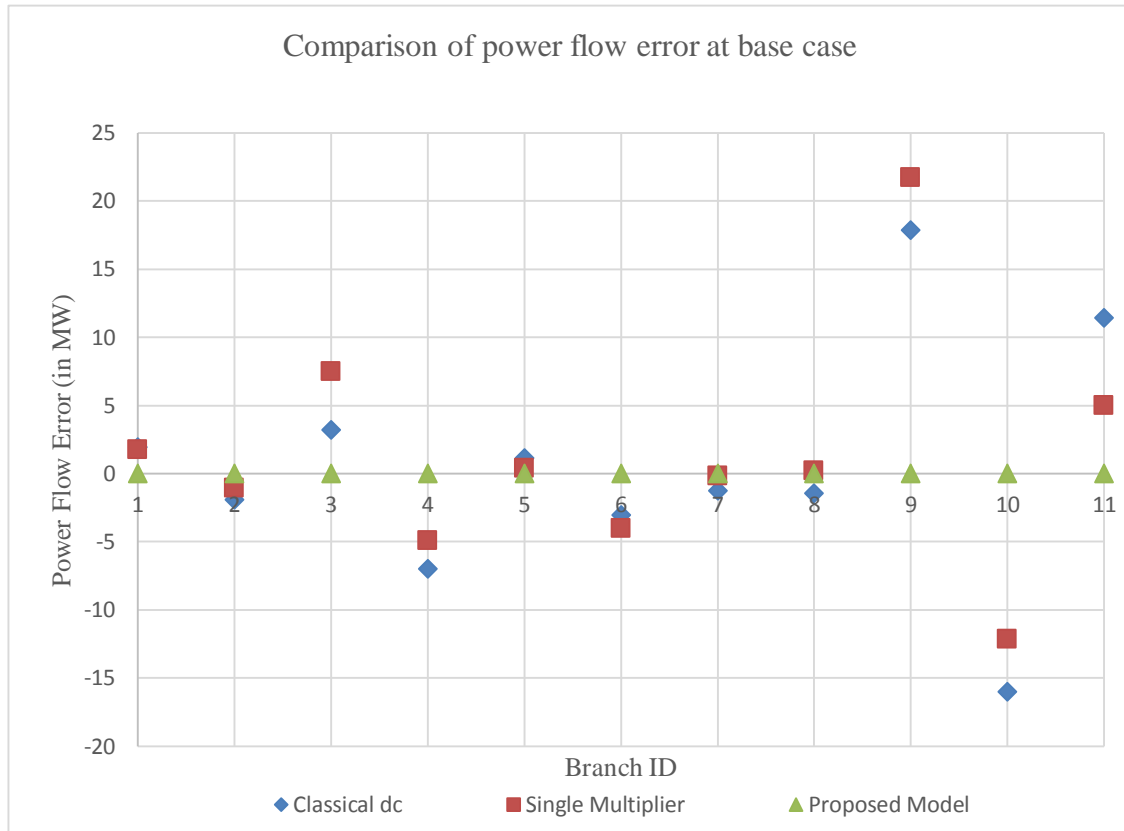Figure 5.3 shows the performance of the models at base operating point.

Figure 5.3 Comparison of power flow errors for different models at base case

It can be seen that there are large MW flow errors for both the classical dc and single multiplier model. However, the proposed model matches the base point power flows to the precision of 10^{-3}. Often, the flow errors are compared in percentage (%) but this unit becomes misleading for branches having small flow because if a small flow, say 1 MW, reverses direction the error in percent can easily be 200%. Therefore, in this work the errors are plotted in MW only.

Also the reactance values are compared for the two cases in Figure 5.4. The
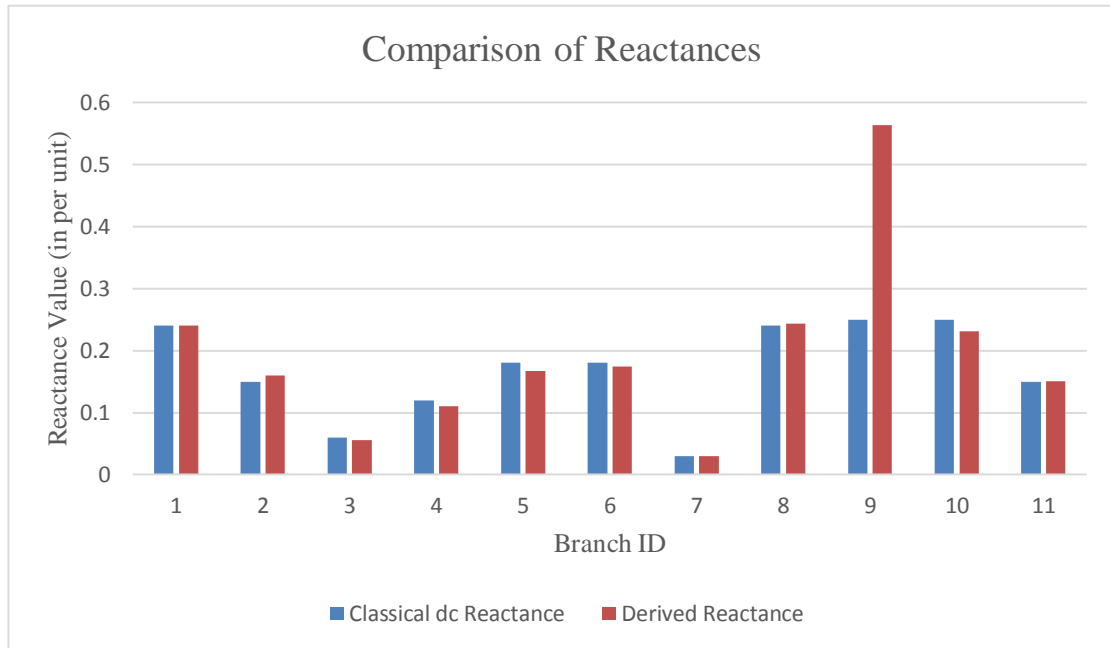

Figure 5.4 Comparison of reactance between different models

reactance value is scaled for the proposed model for purpose of comparison (branch 1

has same reactance value for all models). It is interesting to note that although small

variations appear for most of the branches,, there is a huge variation in reactance for

branch 9, which is high R/X ratio (R/X =1) branch.

The next effort is to examine the difference in the models under contingency

conditions. The models are evaluated for the single branch outage contingency. In this

case each line is removed, one at a time, and the branch power flow is calculated for

each of the dc models and compared to the ac model. Maximum absolute error and root

mean square (rms) flow errors are used as metrics for the analysis.

a) Maximum absolute MW error

It is defined as the maximum of the absolute value of branch power flow error

defined by (5.1). This is computed for each line contingency for the system under study.

Mathematically, it is defined as:

$$Max. \ Absolute \ Error \ (\beta) = \max_{i \in \{1,2,\cdots L\}} [\xi_i]$$

where,

$$\xi_i = \left\| \begin{bmatrix} \left| PF_{aci}^1 - PF_{dci}^1 \right| \\ \left| PF_{aci}^2 - PF_{dci}^2 \right| \\ \vdots \\ \left| PF_{aci}^L - PF_{dci}^L \right| \end{bmatrix} \right\|_\infty$$

PF_{ac}^j = ac power flow on branch j

PF_{dc}^j = dc power flow on branch j

i = Contingency branch ID number

This metric gives an indication of the accuracy of the dc models with respect to ac contingency results.
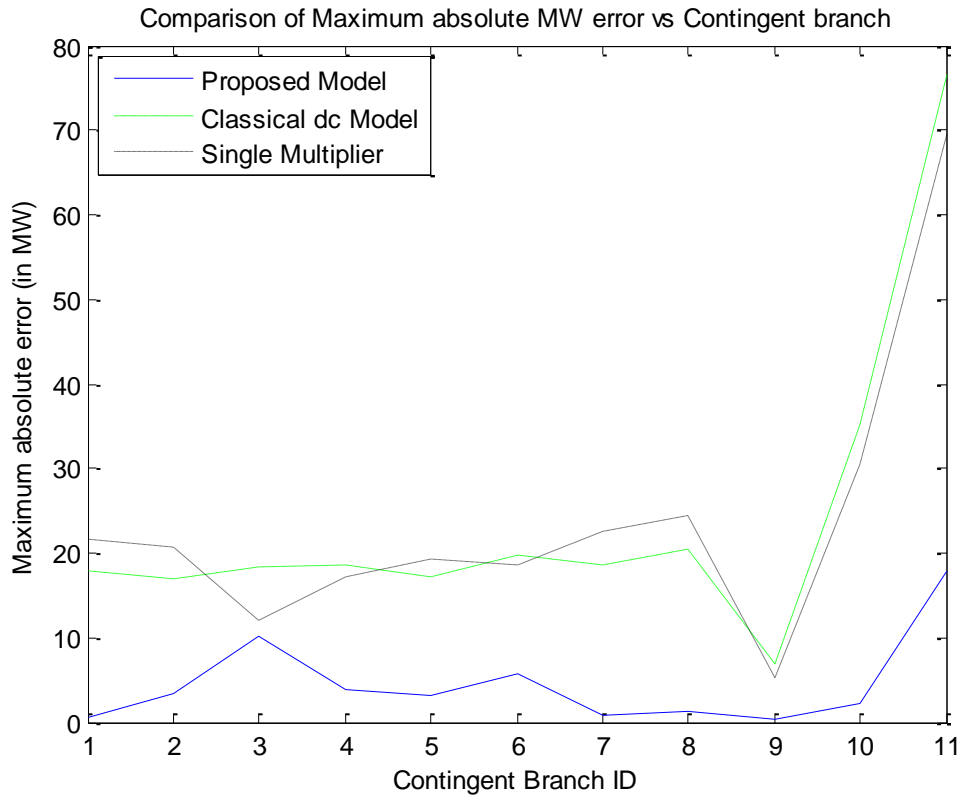
Figure 5.5 Comparison of maximum absolute MW error for contingencies

It can be seen from Figure 5.5 that the proposed model gives better results as compared to the classical dc and single multiplier models. Significant improvements are witnessed on the lines near slack bus and on high R/X ratio branches.

A summative metric, an rms (MW) branch flow error discussed next will provide an overall estimate of error across all branches for each contingency.

b) Root mean square (rms) error estimate

Root mean square is defined mathematically as:

$$RMS \quad Error \quad (\beta) = \sqrt{\frac{\sum_{j=1}^{L}(PF_{model}^{j} - PF_{ac}^{j})^{2}}{L}} \tag{5.4}$$

where,

70

$$L \qquad = \text{Number of branches}$$

$$PF^{j}_{\text{model}} \quad = \text{dc power flow for a given model i.e. classical dc, single multiplier}$$

$$\text{proposed model for branch } j$$

$$PF^{j}_{ac} \qquad = \text{ac power flow for branch } j$$

This measure of error provides the rms flow error (MW) across all the branches for

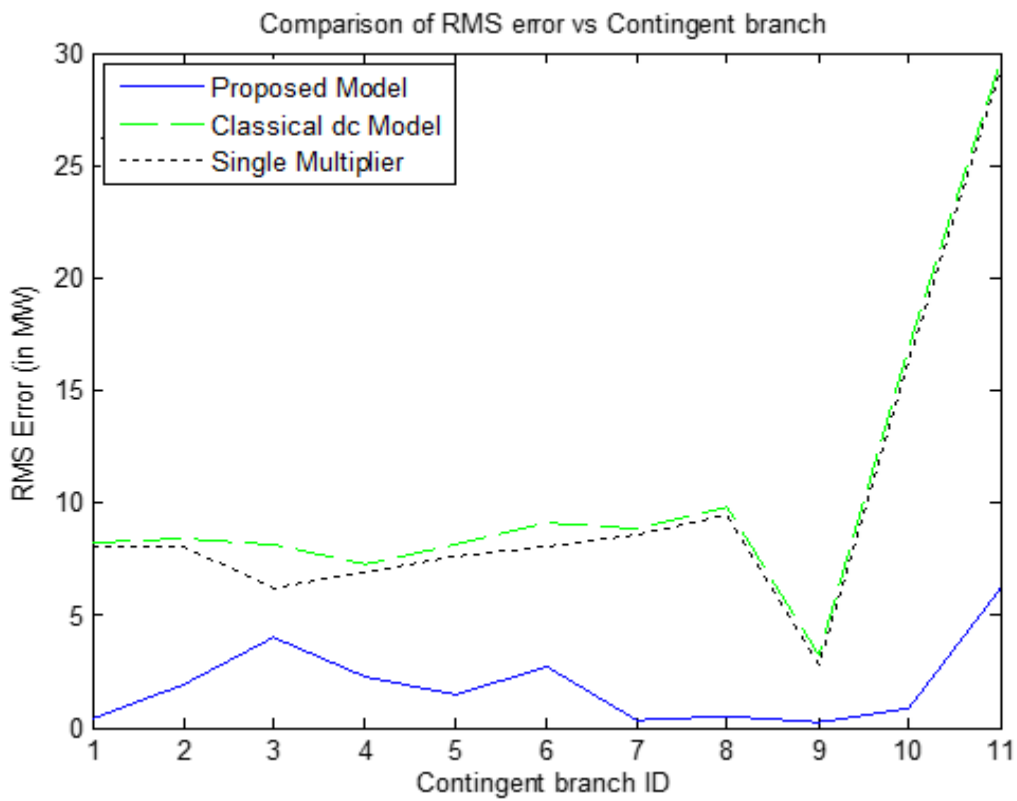a contingency at a particular branch.

Figure 5.6 Comparison of rms error for contingencies

Table 5.8 summarizes the results for 7-bus model which indicates that proposed

model works better than the other two models in terms of both the metrics chosen for

comparison.

Table 5.8 Summary of results for 7-bus model

	Max. Absolute Error (MW)	Max. RMS Error (MW)
Proposed Model	17.84	6.17
Classical DC	76.56	29.61
Single Multiplier	69.51	29.24

5.2.2   Case Study 2: IEEE-118 Bus Model

In this section, the IEEE-118 bus system is examined for the accuracy of dc power flow models (classical dc, single multiplier and proposed model) both at the base case and under single-branch outage contingency conditions. (These are the same numerical experiments performed on the 7-bus model).

It is worthwhile to note that the IEEE-118 bus system has one sub-network (shown in Figure 5.7) that needs to be solved independently (as described in Section 4.5 and Section 4.6) as a sub-problem to obtain the network model.

All the branch power flows obtained from dc models under case operating condition (no contingency) is compared against the ac branch power flow solution. As per (2.13) multiplier for loss compensation is computed to be:

Single Multiplier (γ) = 1.0312

Figure 5.8 Comparison of power flow errors for different models at base case, computed using (5.1) for the IEEE-118 bus system. It can be seen that classical dc model has large errors at the base case. Since the single multiplier accounts largely for

losses, the branch flow errors are comparatively low. Our proposed method matches the
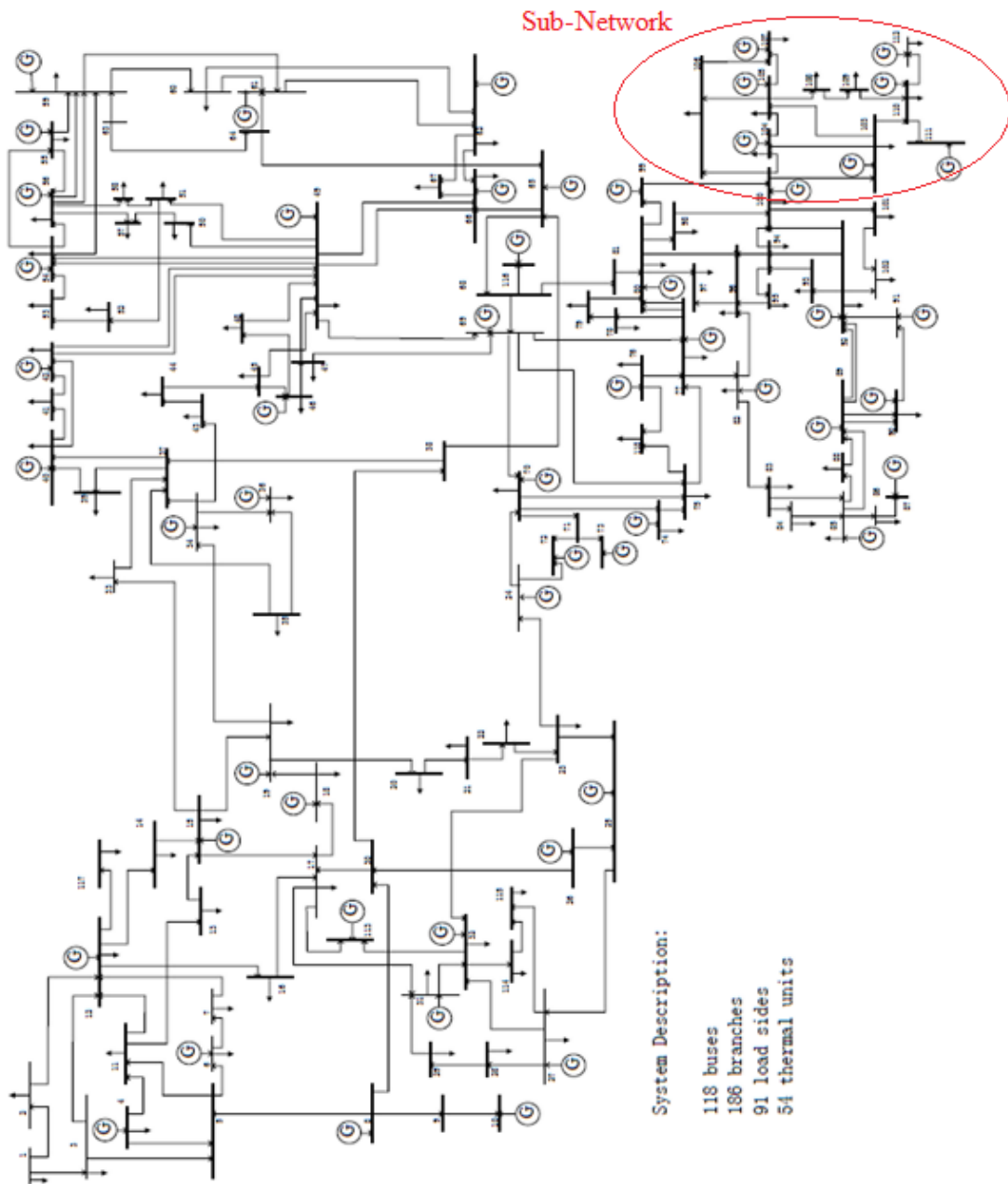
base case with the precision of 10^{-3}.
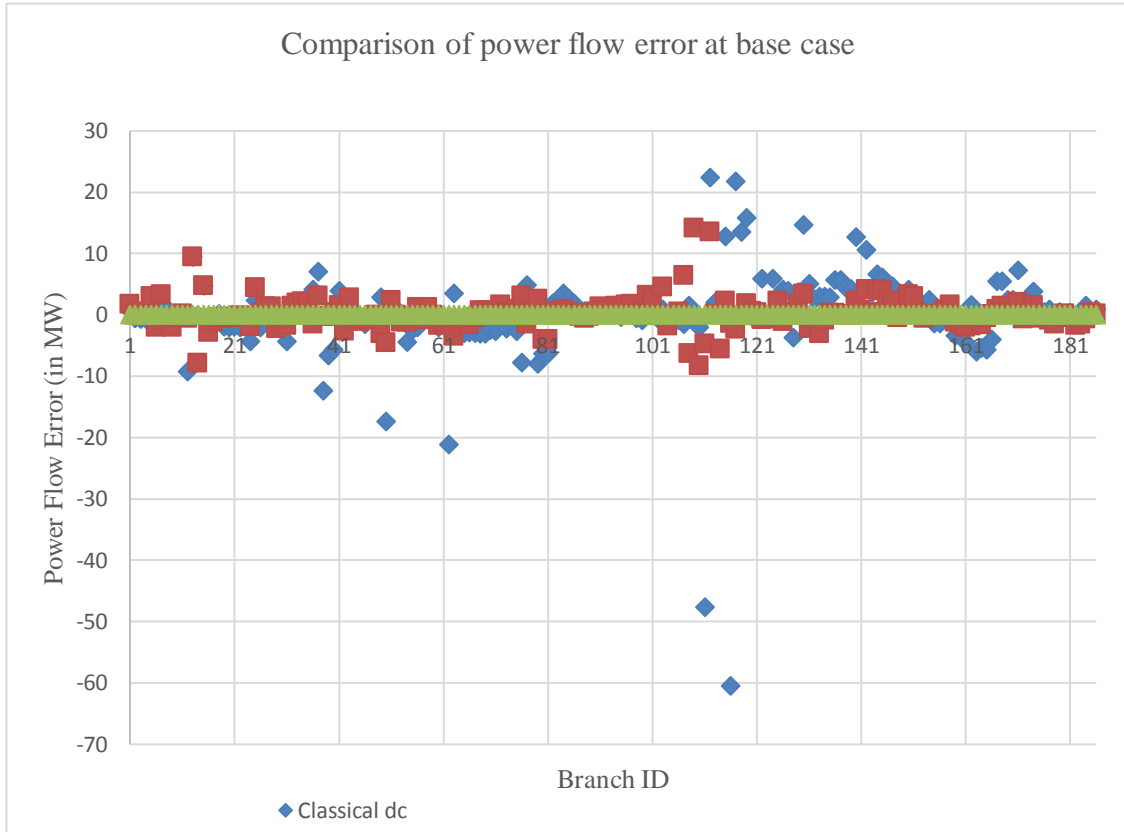

Figure 5.7 IEEE-118 bus Model

Figure 5.8 Comparison of power flow errors for different models at base case

Figure 5.9 and Figure 5.10 illustrate the maximum absolute MW error (using (5.2)). It becomes quite clear from the error duration curve (Figure 5.10) that the proposed model has significantly lower errors as compared to the contemporary methods.
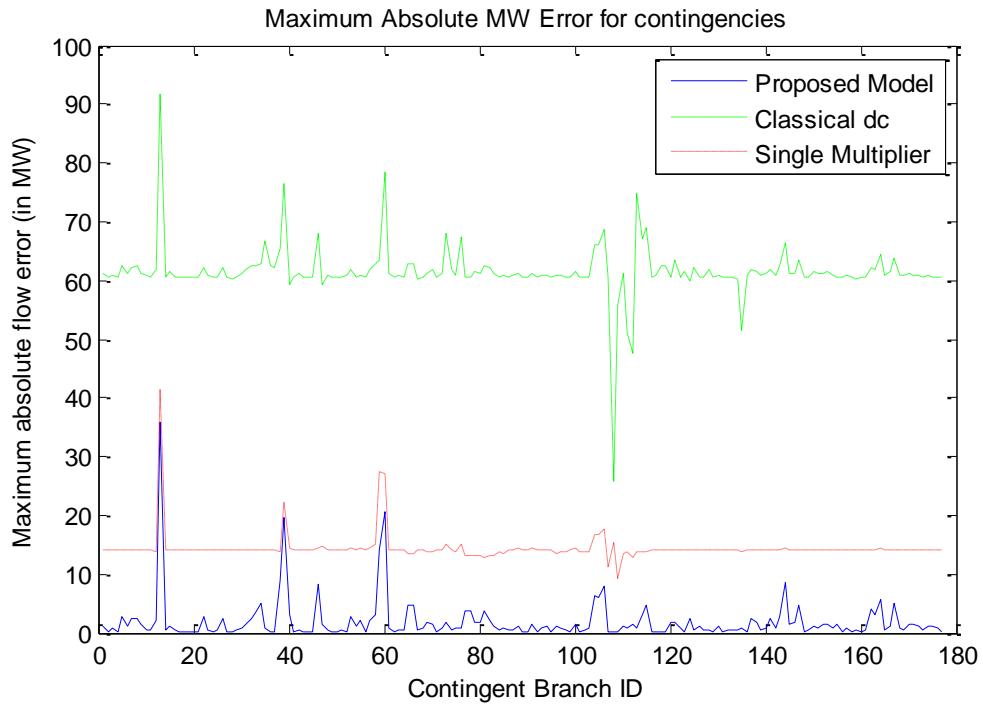
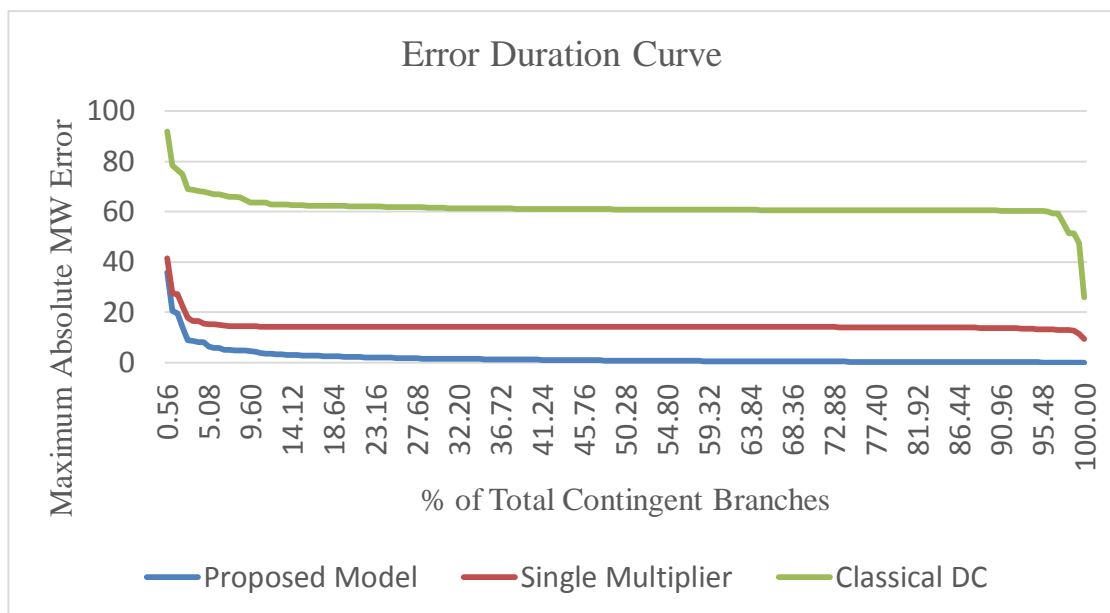Figure 5.9 Comparison of maximum absolute MW error for contingencies

Figure 5.10 Error Duration Curve for maximum absolute MW error for contingencies

Figure 5.10 shows that, for 10% of the branch contingencies, the maximum absolute branch flow error exceeds 4.2MW, 14.35MW and 63.6MW for proposed, single multiplier and classical dc model respectively. Figure 5.11 illustrates the RMS

75

error across all the branches in the network for each specified contingency. It is
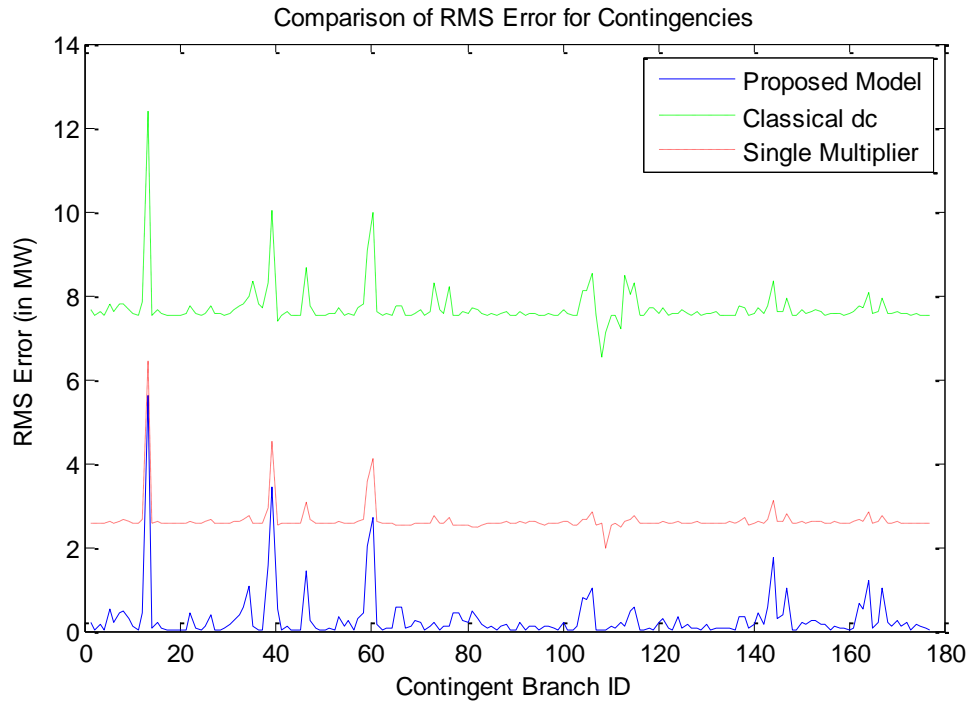
obtained using (5.4).

Figure 5.11 Comparison of RMS error for contingencies

Branch-flow error results for IEEE-118 bus system are summarized in Table 5.9.

Table 5.9 Summary of results for IEEE-118

	Max. Absolute Error (MW)	Max. RMS Error (MW)
Proposed Model	35.95	5.62
Classical DC	91.81	12.40
Single Multiplier	41.36	6.41

5.2.3   Case Study 3: ERCOT Interconnection

Electricity Reliability Council of Texas (ERCOT) shown in Figure 5.12 is one of the interconnections in North America which can serve as a realistic test basis for testing the performance of the dc models discussed so far. This practical system offers new challenges in terms of phase-shifting transformers (as discussed in Section 2.1 and Section 2.2). The phase-shift values for the phase-shifters was kept same as in the original network during the network equivalence process of computing the model parameters. Tests similar to 7-bus and IEEE-118 were conducted on ERCOT interconnection for performance measurement.
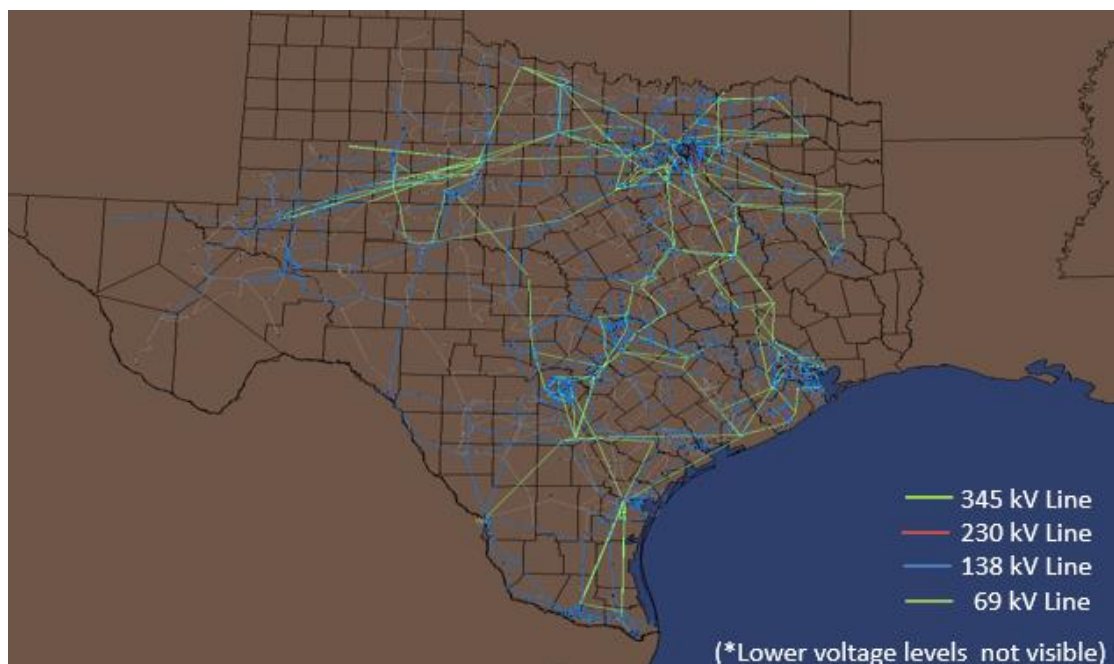

Figure 5.12 ERCOT Interconnection

All the branch power flows obtained from dc models under base-case operating conditions (no contingency) is compared against the ac branch power flow solution. As per (2.13), the multiplier for loss compensation is computed to be:

Single Multiplier (γ) = 1.0212

It is worthwhile to note that branch '6160' is connected to slack bus and branch number in the range 6000-6500 are in the vicinity of the slack bus. It can also be seen from Figure 5.13 that the flow errors for classical dc case tend to accumulate near slack bus. Also, the radial line '6160' connecting the slack bus with the rest of the system incurs the maximum error due to the no loss compensation assumption. . As in previous cases, the proposed model matches the solved ac solution at base case.

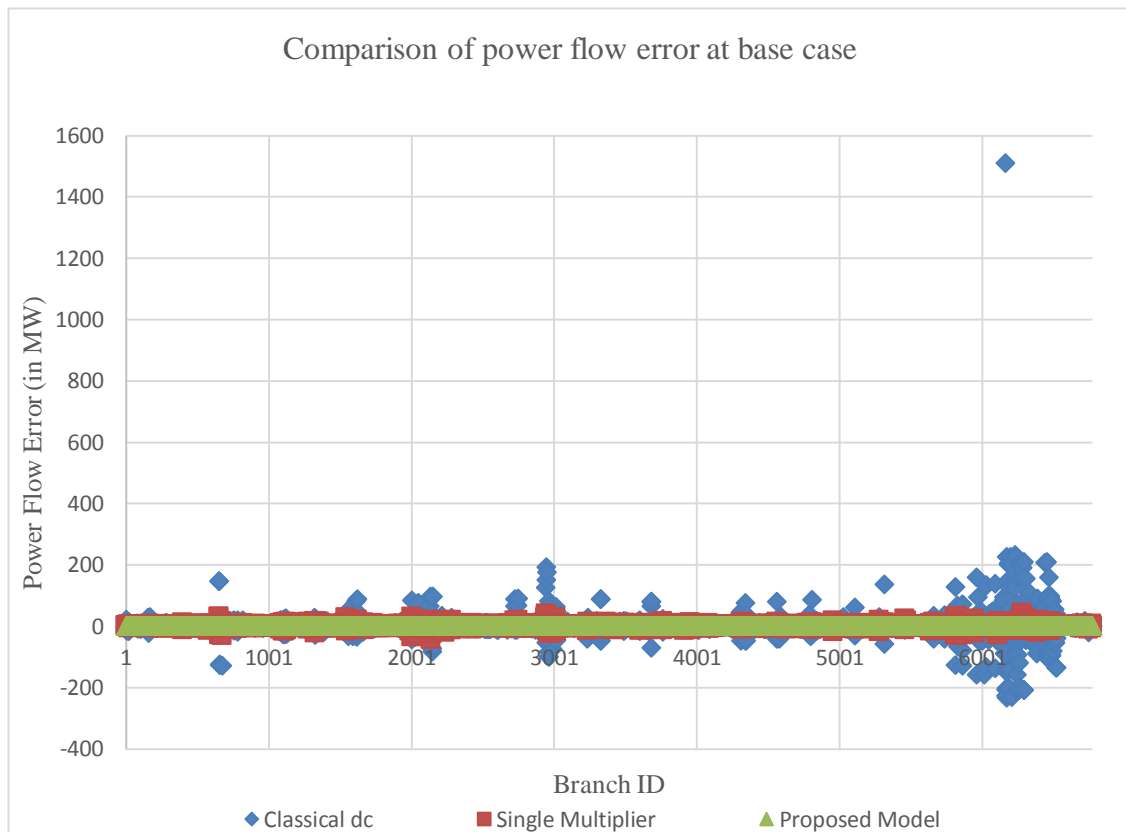Figure 5.13 Comparison of power flow errors for different models at base case

The same metrics as defined for the 7-bus and IEEE-118 test systems are used to evaluate the performance of dc models for ERCOT interconnection under contingency conditions.
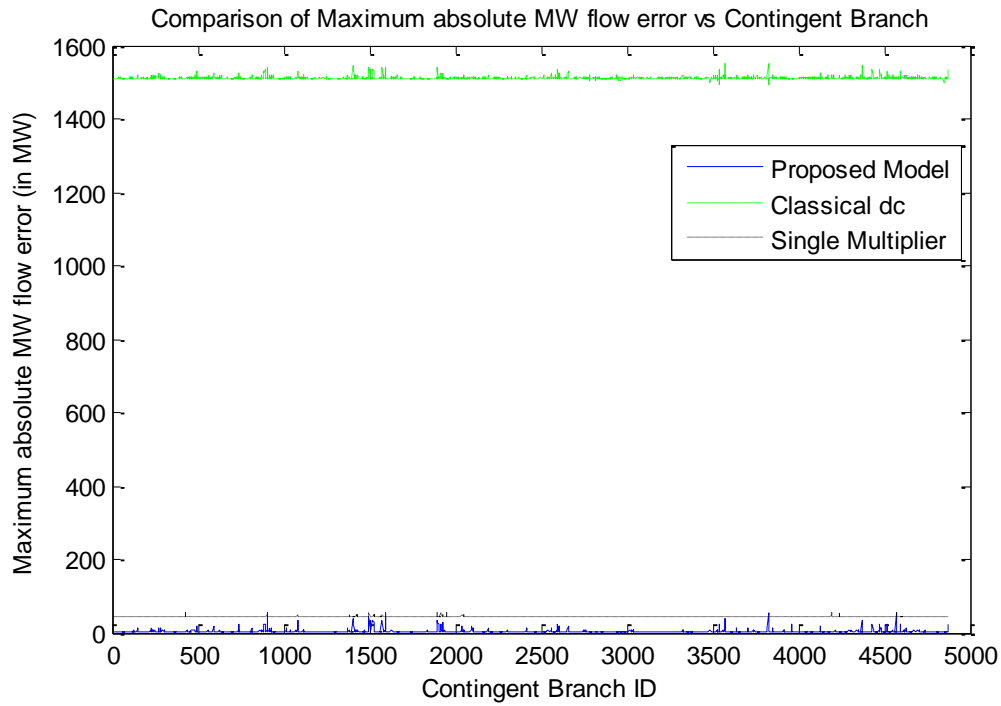
Figure 5.14 Comparison of maximum absolute MW error for contingencies
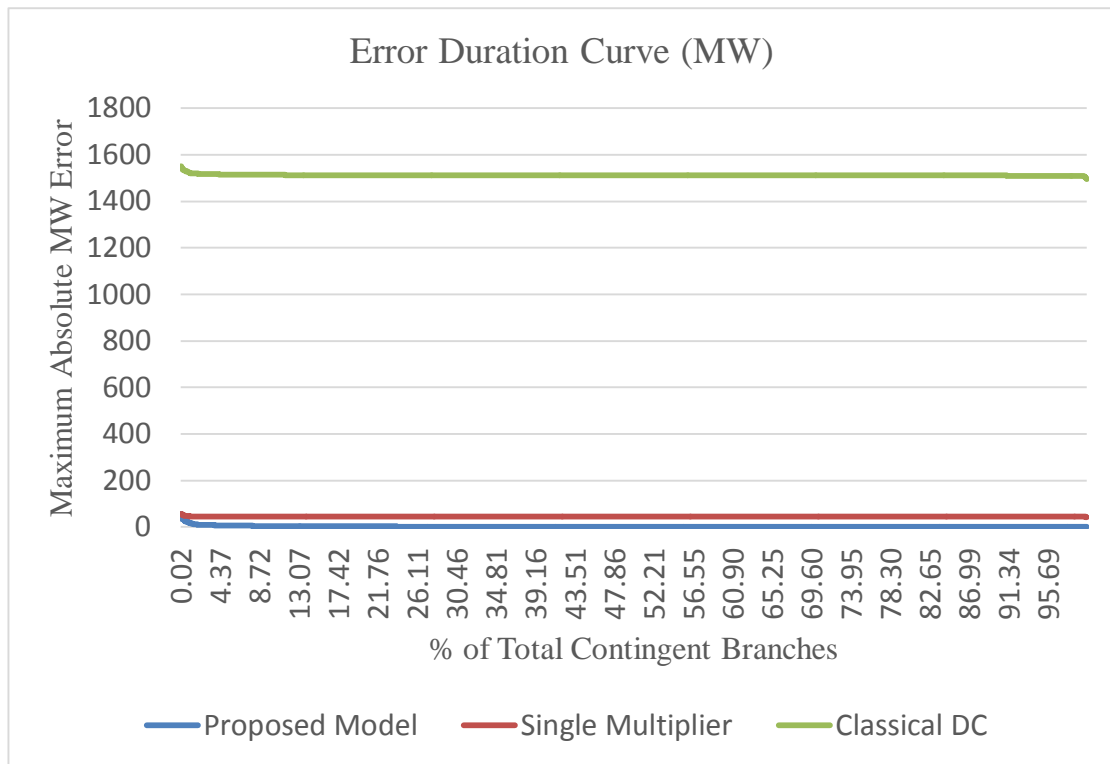
Figure 5.15 Error Duration Curve for maximum absolute MW error for contingencies

Also, it can be seen from Figure 5.14 and Figure 5.15 that the proposed model in general has lower errors compared to the other two models. Figure 5.15 shows that, for 10% of the branch contingencies, maximum absolute MW flow error exceeds 3.96MW, 44.77MW and 1513.36MW for proposed, single multiplier and classical dc model respectively. Figure 5.16 illustrates the RMS error across all the branches in the network for each specified contingency. It is obtained using (5.4).

Figure 5.16 Comparison of RMS error for contingencies

Branch-flow error results for the ERCOT interconnection are summarized in Table 5.10.

Table 5.10 Summary of results for ERCOT Interconnection

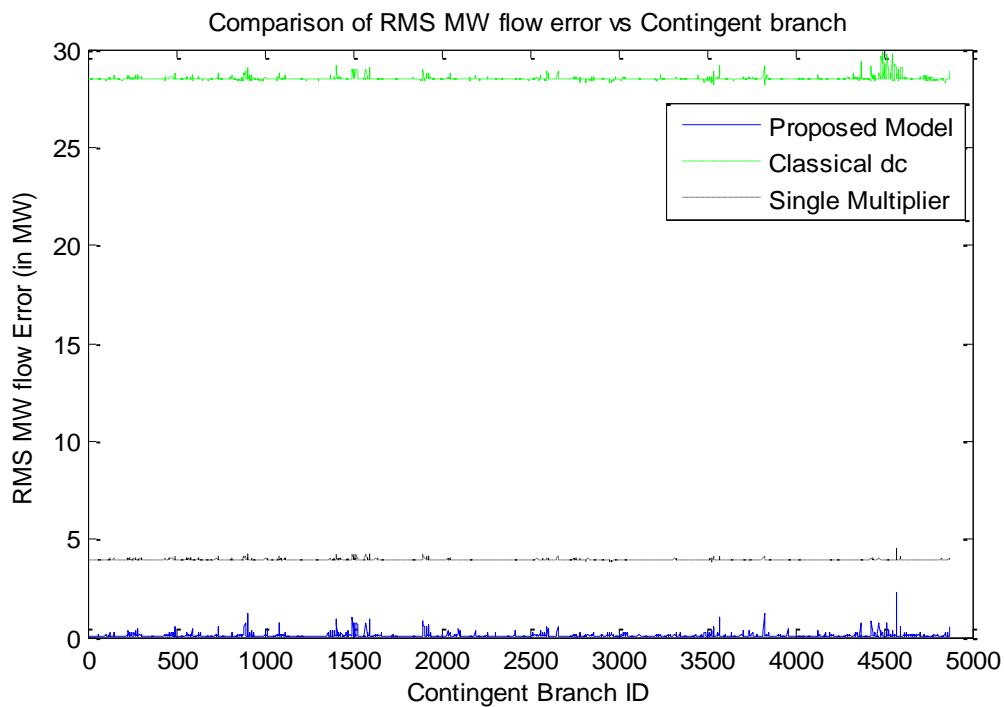|	Max. Absolute Error (MW)	Max. RMS Error (MW)
Proposed Model	54.90	2.27
Classical DC	1551.53	29.82
Single Multiplier	56.60	4.53

It may appear from the results presented in Table 5.10 that the maximum absolute branch flow error is nearly same for both the single multiplier and proposed models. But Figure 5.15 suggests that such instances of comparable maximum absolute branch power flow errors between the single multiplier type dc model and the proposed model are few. .Also, the proposed model achieves a 50% reduction in rms error compared to single multiplier model.

In summary, the proposed model gives better performance indices under both base-case and contingency conditions.

6 CONCLUSION AND FUTURE WORK

6.1 CONCLUSION

In this research work, the most common dc models were introduced and their performance was evaluated numerically. Also, an optimization-based novel dc power flow method in conjunction with the α-matching method was proposed, tested and implemented. The following conclusions are drawn from the work:

In the state independent models, like the classical dc model, the branch flow errors are quite high. A major cause of this error is the lack of loss compensation. The impact of this assumption was not significantly for small systems where the overall system losses are low, but, this effect was magnified for the larger system especially on branches near the slack bus. This effect is clearly visible from the results presented in Section 5.2 and is attributed to the fact that for a large system losses were quite significant.

On the other hand, the state dependent models were derived from the solved ac base case solution and involve different loss compensation techniques. The proposed model was based on an optimized reactance value (obtained using PTDFs) and models loss components as localized power injections. Whereas, the single multiplier models loss by scaling the loads by a uniform factor.

In the proposed model, problems of numerical ill-conditioning were witnessed when solving for network parameters for larger systems which involved radial lines and sub-networks. This was attributed to specific topological features of the system under

consideration. Several examples were illustrated to develop the intuitive understanding of rank deficiency in the Λ-matrix. Furthermore, handling of such ill-conditioning issues by fixing the reactance value for the radial lines and deriving the network parameters for sub-network was described in detail.

Accuracy of all the dc models was evaluated using different test systems: 7-bus, IEEE-118 and 5650-bus Electricity Reliability Council of Texas (ERCOT). Performance of these dc models under base-case and contingency situations was evaluated numerically. Two metrics i.e., maximum absolute branch flow error and rms flow error for each contingency was considered. It was found that the proposed model not only matches the base case to a precision of 10^{-3} but also performs well compared to other dc models under contingency situations.

6.2   FUTURE WORK

This research work was focused on development of a dc model that can match an ac solution as closely as possible, both under base-case and contingency situations. To improve the versatility of this proposed model the following work is suggested for the future:

➢ In the proposed algorithm, the Λ-matrix is of dimension $N.L \times L$ which is computationally quite inefficient in terms of its formation and storage requirements especially for a large systems like eastern interconnection (EI) even if the matrix is sparse. For example, a system of the size of ERCOT which has 5650 buses and 6771 branches the Λ-matrix has approximately 38 million rows. It has been observed in the

construction of this Λ-matrix that there are quite a large number of linearly dependent rows and few rows are very small in magnitude. Therefore, a considerable size reduction can be achieved in the Λ-matrix if these smaller coefficient rows are neglected and hence reduction in computational time.

➢ It can be seen from the results presented in chapter 5 that there are still significant deviations in branch flows from the ac solution for certain contingencies. Therefore, other methods for obtaining the *H* parameters can be investigated to obtain better power flow results. Since the proposed model uses an iterative algorithm based on an initial point estimate, it is subjected to non-convergence issues. It would be interesting to observe the robustness of the proposed algorithm on different test cases.

➢ Since the dc models are quite prevalent in electric-power-market applications, the proposed dc model could be tested for locational marginal price (LMP) comparison and how well this model replicates the congestion in the network.

REFERENCES

[1] U.S. Environmental Protection Agency, "Inventory of U.S. Greenhouse Gas Emissions and Sinks: 1990 - 2012," April 2014, [Online]. Available: http://www.epa.gov/climatechange/Downloads/ghgemissions/US-GHG-Inventory-2014-Main-Text.pdf

[2] U.S. Energy Information Administration, "Emissions of Greenhouse Gases in the United States 2009", March 2011, [Online]. Available: http://www.eia.gov/environment/emissions/ghg_report/pdf/0573(2009).pdf

[3] Executive office of the president, "The President's climate action plan," June 2013, Available: http://www.whitehouse.gov/sites/default/files/image/president27sclimateactionplan.pdf.

[4] L. Murkowski, "Energy 20/20: A vision for America's energy future", [Online]. Available: http://www.energy.senate.gov/public/index.cfm/files/serve?File_id=099962a5-b523-4551-b979-c5bac6d45698

[5] "Most states have renewable portfolio standards (RPS)", [Online]. Available: http://www.eia.gov/todayinenergy/detail.cfm?id=4850

[6] B. Stott, J. Jardim and O. Alsac "DC Power Flow Revisited," IEEE Transactions on Power Systems, Aug. 2009, vol. 24, no. 3, pp. 1290-1300.

[7] J. D. Glover, M. S. Sarma and T. J. Overbye, "Power System Analysis and Design 5th Edition," Cengage Learning, Stamford, 2012.

[8] R. Kaye and F.F. Wu, "Analysis of linearized decoupled power flow approximations for steady-state security assessment," IEEE Transactions on Circuits and Systems, Jul. 1984, vol. 31, issue. 7, pp. 623-636.

[9] Y. Qi, D. Shi, and D. J. Tylavsky, "Impacts of assumptions on DC power flow model accuracy," North American Power Symposium (NAPS), Sept. 2012.

[10] K. Purchala, L. Meeus, D. V. Dommelen and R. Belmans, "Usefulness od dc power flow for active power flow analysis" Power Engineering Society (PES) general meeting, Jun. 2005, vol. 1, pp. 454-459.

[11] T.J. Overbye, X. Cheng and and Y. Sun, "A comparison of the AC and DC power flow models for LMP calculations," Proceedingd of the 37th annual Hawaii international conference on system sciences, Jan. 2004.

[12] B.F. Wollenberg and W.O. Stadlin, "A real time optimizer for security dispatch," IEEE Transactions on Power Apparatus and Systems, Sept. 1974, vol. PAS-93, Issue. 5, pp. 1640-1649.

[13] V. Sarkar and S.A. Khaparde, "A comprehensive assessment of the evolution of financial transmission rights," IEEE Transactions on Power Systems, Nov. 2008, vol. 23, no. 4, pp. 1783 - 1795.

[14] A.J. Wood and B.F. Wollenberg, *Power Generation, Operation and Control*. New York: Wiley, 1996.

[15] H. Oh, "A new network reduction methodology for power system planning studies," IEEE Transaction Power System, May 2010, vol. 25, no. 2, pp. 677 - 684.

[16] X. Cheng and T.J. Overbye, "PTDF – based power system equivalents," IEEE Transaction Power System, Nov. 2005, vol. 20, no. 4, pp. 1868 - 1876.

[17] D.Shi and D.J. Tylavsky, "An improved bus aggregation technique for generating network equivalents," IEEE PES General meeting, July 2012.

[18] R. Baldick, K. Dixit and T.J. Overbye, "Empirical analysis of the variation of distribution factors with loading," IEEE PES General meeting, Jun. 2005, vol. 1, pp. 221–229.

[19] R. Baldick, "Variation of distribution factors with loading," IEEE Transactions on Power Systems, Nov. 2003, vol. 18, no. 4, pp. 1316-1323.

[20] M. Liu and G. Gross, "Effectiveness of the distribution factor approximations used in congestion modeling," Proceedings of the 14th Power System Computation conference, Jun. 2002.

[21] J.J. Grainger and W.D. Stevenson, Jr., *Power System Analysis*, McGraw-Hill, 1994.

[22] P. Yan and A. Sekar, "Study of linear models in steady state load flow analysis of power systems," Power Engineering Society winter meeting, 2002, vo1.1, pp. 666-671.

[23] Western Electricity Coordinating Council (WECC), "WECC 10-year regional transmission plan summary," Sept. 2011. [Online]. Available: http://www.wecc.biz/library/StudyReport/Documents/Plan_Summary.pdf

[24] D.V. Hertem, J. Verboomen, K. Purchala and R. Belmans, "Usefulness of dc power flow for active power flow analysis with flow controlling devices," 8th IEE International conference on AC and DC transmission, Mar. 2006, pp. 58-62.

[25] S. Nagalakshmi, S. Kalyani, V.A. Shobana and R.N. Ranjeni, "Estimation of available transfer capability under normal and contingency conditions in deregulated electricity market," International conference on advances in engineering, science and management (ICAESM), Mar. 2012, pp. 453.459

[26] F. Dorfler and F. Bullo, "Novel insights into lossless ac and dc power flow," IEEE PES general meeting, July 2013, pp.1-5.

[27] D. Chatterjee, J. Webb, Q. Gao and M.Y. Vaiman "N-1-1 ac contingency analysis as a part of NERC compliance studies at Midwest ISO," IEEE PES transmission and distribution conference, Apr. 2010, pp. 1-7.

[28]NERC, Transmission Planning (TPL) Standards. [Online]. Available: http://www.nerc.com/files/TPL-002-0.pdf

[29] NERC, Transmission Planning (TPL) Standards. [Online]. Available: http://www.nerc.com/files/TPL-003-0.pdf

[30] NERC, Transmission Planning (TPL) Standards. [Online]. Available: http://www.nerc.com/files/TPL-004-0.pdf

[31] Z.X Han, "Phase Shifter and Power Flow Control," IEEE Transaction on power apparatus and systems, Oct. 1982, pp. 3790 – 3795.

[32] T. Overbye, "Lecture Notes on Advanced Power Flow Topics," Large Scale Integration of Power System, Fall 2013.

[33] P.E Rylatt and G.J. Cokkinides, "A method for planning phase-shifting transformers using linearized networks sensitivities," IEEE Southeastcon ' 89 Proceedings: Energy and Information technologies in the southeast, Apr. 1989, vo1.2, pp. 832-836.

[34] X. Li and X. Yu, "A generalized power transfer distribution factor for power injection analysis of power grids," IEEE Industrial Electronics Society IECON, Oct. 2012, pp. 4724-4728.

[35] D. J. Tylavsky, "Lecture Notes on Computer Solutions of Power Systems," Fall 2012.

[36] Strang, Gilbert. *18.06 Linear Algebra, Spring 2010*. (MIT OpenCourseWare: Massachusetts Institute of Technology), http://ocw.mit.edu/courses/mathematics/18-06-linear-algebra-spring-2010 License: Creative Commons BY-NC-SA.

[37] Y. Qi, "Network reduction for power system planning," Nov. 2013, Master's thesis, School of Electrical, Computer and Energy Engineering, Arizona State University, pp. 46-48.